Chemical Reviews

Theoretical Models for Solvated Electrons

DA-FEI FENG and LARRY KEVAN*

Department of Chemistry, Wayne State University, Detroit, Michigan 48202

Contents

1. Introduction

The understanding of electron localization and solvation in liquids and glassy disordered media is a fundamental problem in the chemistry and physics of condensed phases. This problem is particularly relevant to a variety of chemical areas, including charge conduction in dielectrics, radiation chemistry, and electron transfer in condensed phases. The wide interest and relevance of electron solvation are related to the fact that these "excess" electrons are solvated in a variety of polar and nonpolar media and are highly reactive.[1] Optical, photoconductivity, and electron magnetic resonance techniques have been most exploited to develop an experimental description of solvated electrons. Early optical spectroscopic data showed that solvated electrons are characterized by a broad, asymmetric, and structureless band. The position of this band depends on the medium but generally falls in the visible and near-infrared spectral regions. The optical absorption band and the wavelength dependence of the photocurrent determine the general features of the energy level structure of excess electrons in various media.[2] Structural information has been obtained by electron spin resonance (ESR). The ESR line for the solvated electron consists of a single, inhomogeneously broadened line at a g value that is very close to that for the free electron. This suggests that the electron
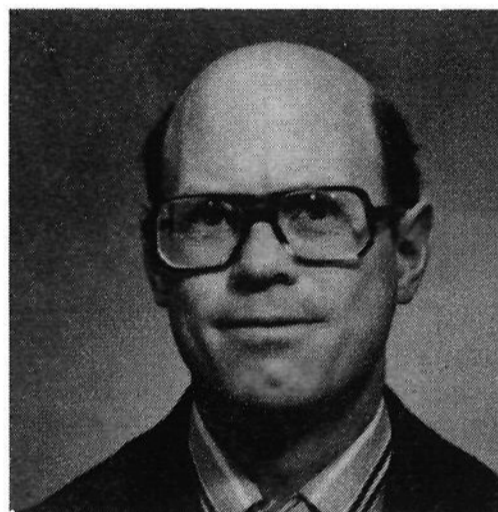
Larry Kevan is Professor of Chemistry at Wayne State University. He received his Ph.D. with Willard F. Libby at the University of California at Los Angeles in 1963, did postdoctoral work at the University of Newcastle with J.J. Weiss, and taught at the University of Chicago and the University of Kansas before moving to Wayne State in 1969. He has also held visiting appointments at the Danish Atomic Energy Research Establishment, University of Utah, Institute of Chemical Kinetics in Novosibirsk, USSR, University of Nagoya, Japan, University of Paris, and Hochschule der Bundeswehr in Munich. His research interests involve electron localization and solvation, the development of electron spin–echo spectrometry for structural studies in disordered systems, and the application of electron magnetic resonance relaxation and electron spin double resonance methods to chemical problems.
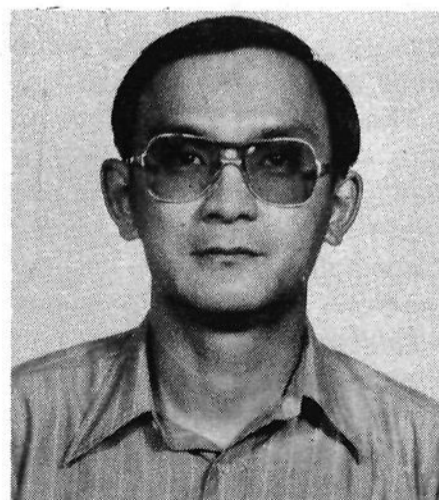
Da-Fei Feng teaches chemistry at San Diego Mesa College. He received his Ph.D. degree in Physical Chemistry in 1973 from Wayne State University with Larry Kevan. He and Professor Kevan worked closely with Professor Kenji Fueki of Nagoya University to develop a semicontinuum model for solvated electrons. He also worked with William Hase on classical trajectory calculations and did postdoctoral work in this area with Jack Root at the University of California at Davis. His research interests lie in solvated electron theory, classical trajectory calculations, and ion interactions in polar solutions.

is trapped in a potential well surrounded by a number of symmetrically oriented solvent molecules. By analysis of second-

moment ESR line shapes, forbidden spin-flip satellite transitions, electron spin–echo modulation patterns, and pulse radiolysis data, a detailed description of the electron localization sites and solvation mechanisms has been developed.[3]

Here we review the theoretical models that have been advanced to describe solvated electrons in disordered systems. Electron solvation in polar or nonpolar media has a superficial resemblance to the well-known particle-in-a-box problem. Early theoretical models attempted to describe the interactions between the electron and the solvent molecules in terms of a spherical box type potential.[4] These models do not give good agreement with experimental results even with the box size as a parameter. These models emphasize the short-range interactions. These are very important but are not sufficient.

An adequate description of the solvated electron problem must include both short- and long-range interactions to properly describe the role the medium plays. In principle, an ab initio molecular orbital (MO) theory would "solve" the problem of electron solvation. This is true only if a sufficient number of solvent molecules are included in the model since here we are dealing with liquid and glassy disordered states. Unfortunately, this number of molecules seems to be very large and is beyond the scope of present day computational methods. Thus far, the largest system that has been treated by ab initio methods consists of five water molecules plus an electron (41 electrons).[5] As we will see later, the excess electron density even in polar media extends into the second solvation shell. Furthermore, even more distant molecules are polarized by the electron charge. Therefore, a realistic theoretical model must include more molecules than is practical with present day ab initio methods.

The ab initio method has thus far only been used to investigate short-range interactions.[6] Even then, these calculations are extremely expensive. A number of approximate molecular orbital methods such as CNDO and INDO[7] have been used by several research groups.[8] Unfortunately, these methods are also limited in the number of solvent molecules they can handle and therefore emphasize the short-range interactions.

Long-range interactions are emphasized in the continuum model which uses the concept of polarization from classical electrostatics to obtain a potential. This potential is used with a hydrogenic wave function and the quantum mechanical variational principle to treat electron solvation in polar media.[9] Both adiabatic and self-consistent-field (SCF) approximations have been used to effectively reduce an N-electron problem to a one-electron system. In the adiabatic approximation the excess electron is assumed to be moving slower than the solvent molecule electrons, while in the SCF approximation the excess electron is assumed to be under the average influence of all other electrons. The methods of calculation using these two approximations are very similar. The whole medium is represented by the static and optical dielectric constants and the potential has the form of r^{-1} mediated by the medium properties. The amount of computation involved in this model is tractable, and the model can easily be adapted to various polar systems. However, the experimentally observed optical absorption maximum is reproduced by parameterizing a cavity radius for the solvated electron so no *prediction* of experimental data is achieved. In addition, the continuum model does not even account for the stability of solvated electrons, primarily due to the neglect of the short-range interactions between the electron and the nearest solvent molecules.

Attempts to include both short- and long-range interactions led to the semicontinuum model[10,11] which builds on the continuum model by introducing a fixed number of symmetrically situated solvent molecules in the first solvation shell and short-range electron–solvent interactions. This adds a few medium-dependent parameters which can be measured experimentally. The semicontinuum model is more molecular in

nature, but computationally it is still about as simple as the continuum model. The semicontinuum model has been applied to a large number of different systems under different conditions, with results that compare favorably with those observed in experiments.[1,12] The model has also been extended to explain excess electron solvation in nonpolar systems with reasonable success.[13] The semicontinuum model has been made more rigorous by incorporating an ab initio framework to treat the short-range interactions.[5] The basic physical picture regarding solvated electrons provided by the semicontinuum model seems to be sound. However, the particular formulation of the short- and long-range interactions[14] and the balance between them require further improvement to better explain all existent experimental data.

In this review we describe molecular orbital, continuum, and semicontinuum models of electron solvation, including recent attempts to improve on these different approaches. Finally, several current problems that do not seem to be satisfactorily treated by these models are discussed.

2. Molecular Orbital Models

As mentioned in the introduction, molecular orbital methods are good at providing information concerning interactions that are short-ranged, particularly where the overlap of orbitals is significant. Whether the electron is localized on a single atom or delocalized over several atoms can be seen directly from the calculated spin density on each atom. Furthermore, it has been demonstrated that molecular orbital methods account quite successfully for the variation in excitation energy observed experimentally for the solvated electron in mixtures such as water and ammonia.[8b]
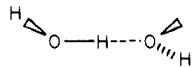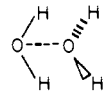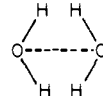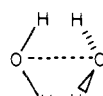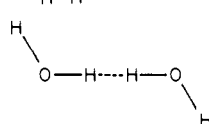
The solvated electron is an open-shell problem. It is therefore inherently a difficult task to be handled by molecular orbital theory. Consider a system such as $(H_2O)_n^-$ where n denotes the number of H_2O molecules strongly interacting with the solvated electron. With approximate molecular orbital methods, CNDO or INDO, n as large as six[15] (the octahedral configuration) has been tried. But a complete ab initio calculation has thus far only been attempted for the dimer model with $n = 2$.[6] It is, however, important to investigate such small systems like the dimer model to check the applicability of the method and the possible importance of dimeric interactions. The results of these studies may serve as a means to simplify more complex interactions encountered in larger systems.

2.1. Dimer Model

Raff and Pohl performed the first semiempirical MO calculation on the solvated electron in liquid ammonia.[16] In their model the electron is assumed to be sandwiched between two protons from the solvent molecule. The wave function is thus approximated to be that of H_2^+. The effect of the solvent is incorporated in the parameter of the trial wave function. If the energy of the isolated dimer molecules is taken as reference level by analogy to H_2^+,[17] the model predicts that the electron is only slightly bound in liquid ammonia and that the ground to excited level transition is really a bound–continuum transition. Electrons are known to be trapped very stably in liquid ammonia, and experimental results also suggest that the excited state for the solvated electron in water is bound.[2] In view of the primitive nature of the model, the poor results are not all that unexpected.

Before proceeding with the discussion we will define two energy notations to facilitate the comparisons of the various calculated results. Let n be the number of solvent molecules S around the electron. $E(nS)$ is then the sum of the energies of n isolated solvent molecules; $E(S)_n$ is the energy of a system composed of n solvent molecules arranged with a specific geometry ($n = 1$, monomer; $n = 2$, dimer; $n = 4$, tetramer; $n =$

TABLE I. Naleway and Schwartz[6] ab Initio Calculations on the Hydrated Electron Using a Dimer Model[a]

conformers	$R(OH)$, Å	$R(OO)$, Å	$E(H_2O)_2$, au	$E(H_2O)_2^-$, au	E_s^1,[b] eV	E_s^2,[c] eV
A.	0.957	2.65	-152.0178	-151.8009	5.90	-1.14
B.	0.957	2.65	-152.0147	-151.7951	5.97	-0.99
C.	0.957	3.18	-151.9947	-151.8415	4.17	-2.25
D.	0.957	3.18	-151.9994	-151.8292	4.63	-1.91
E.	1.16	3.70	-151.9319	-151.8748	1.55	-3.16

[a] $E(2H_2O) = -152.0068$ au, $E(H_2O) + E(H_2O)^- = -151.7588$ au. [b] $E_s^1 = E(H_2O)_2^- - E(H_2O)_2$. [c] $E_s^2 = E(H_2O)_2^- - [E(H_2O) + E(H_2O)^-]$.

5, pentamer; etc.). The charged species of these systems are given by $E(nS)^-$ and $E(S)_n^-$, respectively.

Various other dimeric models have also been suggested without much success. However, the model of Naleway and Schwartz[6] will be discussed before we terminate the discussion on dimeric molecular orbital models. They focused on the hydrated electron system and performed the first ab initio study. Their main purpose was to examine the energetic stability of the electron with two solvent molecules around it. Five different arrangements of the water molecules are considered (see Table I). Groups of Gaussian functions[18] were used as the basis set; they have been applied quite successfully to the study of ground-state energies for a range of atomic systems.[19] The energy for the dimeric system, $E(H_2O)_2^-$, was calculated as a function of the oxygen–oxygen separation R_{O-O}, but in some cases the O–H bond length R_{O-H} was also varied to attain lower energy. By comparing the values of $E(H_2O)_2$ and $E(H_2O)_2^-$, it is interesting to note that the most stable neutral conformer does not give the most stable charged conformer. Conformer E, which is the one also used by Raff and Pohl,[16] gives the lowest energy for the charged system. Clearly in all cases studied the charged species are unstable relative to $E(H_2O)_2$. The charged species are also unstable with respect to $E(2H_2O)$. However, $(H_2O)_2^-$ is stable relative to the separated H_2O and H_2O^-. Again conformer E gives the maximum stability. It appears that, at least for dimers, the charged species are not as stable energetically as their neutral counterparts, although the difference in energy is small. Also $(S)_2^-$ is stable relative to $S + S^-$. Similar results are obtained when approximate MO methods are used.[8b]

2.2. Tetramer and Pentamer Models

Since experimental evidence gives strong support for a solvation number greater than two, we will proceed directly to tetramer models. In view of the complexity involved in the calculation when four or more solvent molecules are around the electron, researchers who attempted this problem all resorted to approximate molecular orbital theory. CNDO and INDO methods, which essentially involve solving the Hartree–Fock self-consistent-field (SCF) equations with varying degrees of approximation, have been used.

Using the CNDO method Weissmann and Cohan[8d] examined the situation when four and five water molecules surround the
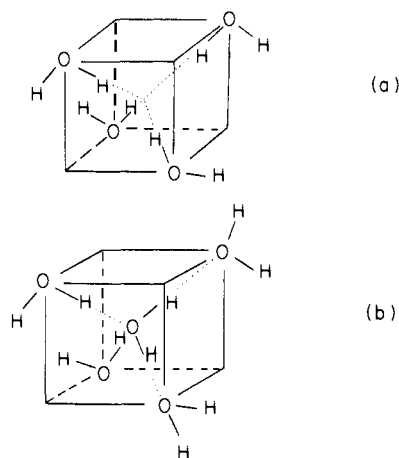
Figure 1. Tetramer (a) and pentamer (b) models for the hydrated electron used by Weissmann and Cohan.[8d]

TABLE II. Weissmann and Cohan[8d] CNDO Calculations on the Hydrated Electron, $(H_2O)_n^-$

n	geometry[a]	$E(H_2O)_n^- - E(H_2O)_n$, eV	E_{HO}^-,[b] eV
1		0.65	0.65
4	tetramer	-0.52	-0.39
5	pentamer	-0.84	-0.57

[a] See Figure 1 for geometrical structures. [b] The highest occupied orbital energy of the charged system.

solvated electron. The structures of these models are shown in Figure 1 and some of the results are included in Table II. It is interesting to note that as the number of H_2O molecules around the solvated electron is increased, $E(S)_n^- - E(S)_n$ becomes more negative, which means that the system becomes more stable. Based on this result Weissmann and Cohan[8d] argued that the normal ice structure (Figure 1b) is a more likely configuration for the hydrated electron that the tetrahedral structure. Such a hydrogen-bonded icelike cluster is also predicted by Ray.[20] However, the experimental results do not support this type of

TABLE III. Howat and Webster[8b] INDO[a] Calculations on the Hydrated and Ammoniated Electron with a Tetrahedral Model

S	R, Å	$E(S)_4$, au	$E(S)_4^-$, au	$E(4S)$, au	$E(3S) + E(S)^-$, au	SD,[b] eV	ΔE,[c] eV
H_2O^d	0.95	-77.008	-76.8241	-77.0076	-76.7424	-2.22	2.08
NH_3^e	1.70		-53.8888	-54.1196	-53.8652	-0.64	0.72

[a] Valence basis set is used. $E(H_2O) = -19.252$ au, $E(H_2O)^- = -18.987$ au, $E(NH_3) = -13.5299$ au, $E(NH_3)^- = -13.2756$ au. [b] $SD = E(S)_n^- - E((n-1)S) + E(S)^-$, stability criterion. [c] Energy difference between the lowest unoccupied and highest occupied molecular orbitals. [d] OH-bond-oriented tetrahedral model as in Figure 2a. [e] Molecular-dipole-oriented tetrahedral model as in Figure 2c.
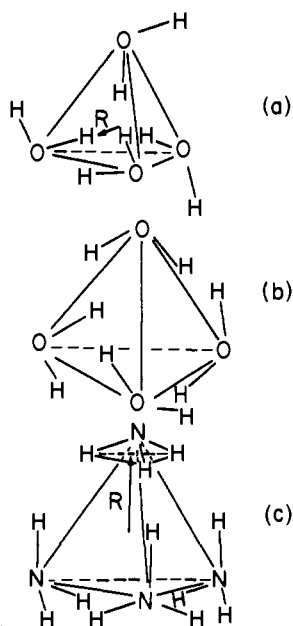

Figure 2. Bond–dipole (a) and dipole-oriented (b, c) tetrahedral models for the hydrated and ammoniated electron used by Howat et al.[6b] and Ishimaru et al.[15] R is taken as the cavity radius.

Figure 3. Total energy of the hydrated electron using model (a) shown in Figure 2.[6b] The energy reference level is assumed to be the sum of the energy corresponding to $3H_2O$ and H_2O^-.

molecular structure.[2] Also, Newton[5] pointed out in his more extensive calculation that such a structure is not the most stable when the cluster is embedded in a dielectric continuum.

Howat and Webster[8b] and Ishimaru et al.[15] have separately studied the hydrated and ammoniated electron with the INDO approximation. Howat and Webster examined only the tetrahedral model (see Figure 2), while Ishimaru et al. studied a tetrahedral model and an octahedral model. With these models, they examined a series of isoelectronic solvent molecuels: water, ammonia, and hydrogen fluoride. We will limit discussion to the results on e_{aq}^- and e_{am}^- calculated on the basis of the tetrahedral model.

Howat and Webster calculated the total energy of the negatively charged system $E(S)_n^-$ as a function of R for the three configurations shown in Figure 2. For all the configurations a minimum value for $E(S)_n^-$ was found along the R coordinate. Table III shows that e_{aq}^- and e_{am}^- both attain stability relative to $E(3H_2O) + E(H_2O)^-$ but not relative to $E(4H_2O)$. The stabilization energy for the OH-bond-oriented water tetramer (Figure 2a) is -2.2 eV (see Figure 3), while for the molecular-dipole-oriented water tetramer (Figure 2b) it is only -1.63 eV. All detailed results shown for water in the paper are for the OH-bond-oriented model. However, similar comparison in orientations for ammonia was not made. Thus, the validity of comparing the results for OH-bond-oriented water with molecular-dipole-oriented ammonia is not clear. In particular, the R values in Table III are defined differently, as shown in Figure 2, and are not comparable.

Ishimaru et al. also studied the energetics of the e_{aq}^- and e_{am}^- using the same configurations as those shown in Figure 2. They used a larger basis set than Howat et al. but fixed the O–O and N–N distances (2.92 and 3.01 Å) to those determined by X-ray
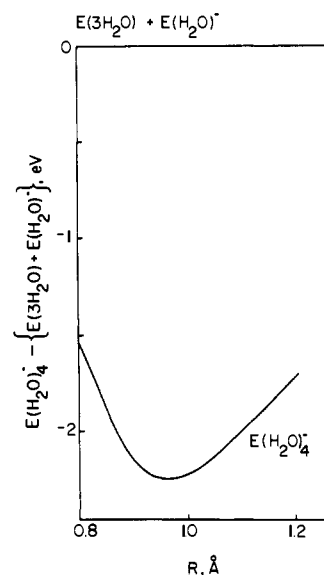
data. These distances are expected to be too large for the stable solvated electron. For all the stable systems the spin density on the protons is calculated to be negative. It would be interesting to use Ishimaru's basis set and perform a calculation similar to that of Howat and Webster and observe the effect of the basis set on the configurational minimum.

Recently Noell and Morokuma[21] studied the hydrated electron in the framework of a fractional charge model. The first solvation shell is treated on the basis of the ab initio method. Second and third solvation shells are included by representing the molecules by functional charges.[22] The two protons and two lone pairs of electrons in each water are simulated by two negative charges Ne^- where e^- is the electronic charge and N is the fractional charge which reproduces the experimental dipole moment of water. The number of water molecules in the second and third shells is determined by forming two hydrogen bonds with each inner shell oxygen. In this calculation only the electronic energy is calculated variationally. The medium rearrangement energies due to surface tension of cavity formation and hydrogen-bond breaking are estimated separately and combined with the electronic energy to get the overall energy.

Two geometries were considered. Geometry A has a tetrahedral first shell with the positive end of each water dipole directed toward the cavity center. The water molecules are oriented so that the total complex has C_{2v} symmetry. There are 8 molecules in the second solvation shell and 16 in the third. Geometry B has an octahedral first solvation shell with one OH bond of each water molecule oriented toward the electron and D_2 symmetry. There are 12 molecules in the second solvation shell and 24 in the third.

Calculations were carried out for the tetrahedral model with the distance from the e^- to the oxygens of the first solvation shell equal to 2.5, 3.0, 3.5, and 4.0 Å. For the octahedral model calculations were made for a single distance, 3.086 Å. For the

tetrahedral model a configurational minimum total energy is found at 3.0 Å. However, the total energetics indicate no stabilization for the electron; the energy required to form the neutral cluster is greater than the stabilization obtained by adding the electron. For example, let us consider the tetrahedral model for $R = 3.0$ Å. The electronic energy required to arrange 4 water monomers into a tetrahedral geometry is 7.7 kcal/mol. Placing an electron in this prearranged cluster lowers the electronic energy by -10.3 kcal/mol. Thus, the electronic energy for the reaction $e^- + 4H_2O \rightarrow (H_2O)_4^-$ is -2.6 kcal/mol. However, the surface tension energy (11.9 kcal/mol) and hydrogen-bond-breaking (22.5 kcal/mol) medium rearrangement energies must be added to get the total energy of this reaction, which becomes 31.8 kcal/mol. Thus, the total reaction is endothermic. The addition of a second and third solvation shell gives 30.4 and >65.3 kcal/mol for the total reaction endothermicity. It is interesting that little extra energy is required to orient the second solvation shell.

It is of interest to evaluate the relative calculated energies of the tetrahedral and octahedral models, although since both are unstable the significance is unclear. The tetrahedral, molecular-dipole-oriented model is favored over the octahedral, bond-dipole-oriented model at $R = 3.0$ Å according to their reaction endothermicities of 31.8 and 54.8 kcal/mol. This result occurs primarily because the neutral tetrahedral conformation requires less energy per molecule to form than the neutral octahedral conformation. However, once the neutral clusters are formed the octahedral cluster binds the electron more tightly than the tetrahedral cluster (-4.94 kcal/mol per molecule vs. -4.68 kcal/mol per molecule). Thus, these calculations suggest that the octahedral model binds electrons more strongly but it is energetically less favorable to construct the neutral oriented cluster.

We recall that the experimental electron magnetic resonance results indicate that the solvated electron in aqueous systems does have an octahedral, OH-bond-oriented configuration. It would be interesting to carry out calculations with the fractional charge model for two different octahedral configurations, one with molecular dipole orientation and the other with bond dipole orientation.

From a second moment[23,25] and spin–echo analysis[26,27] of the ESR spectrum of the solvated electron in alkaline ice glass at 77 K, doped with deuterium and oxygen-17, Schlick et al.[25] found the spin density of the nearest proton to be positive. All the calculations thus far indicate that it is negative.[5,14,21] Noell et al.[21] calculated an unstable trapping system $(H_2O)^-$ and found that the proton spin density for this configuration is positive. Based on this, the authors suggested that for electrons trapped in very shallow potentials it is possible to see positive spin densities on the protons due to extensive spin delocalization. Ishimaru et al.[14b] found that under certain conditions a positive spin density on the proton is obtained (see the results for model I obtained by method I in Table V of ref 14b). However, no attempt was made to distort the first shell water molecules and decrease the potential to explore this problem. It is interesting that Ishimaru et al.[14b] did find positive spin densities for one of their calculational methods but rejected it because they thought the spin densities should be negative. This discrepancy between experiment and theory remains unresolved.

Some observations can be made on the results for the solvated electron obtained from molecular orbital treatments. (1) The solvated electron is not calculated to be stable relative to one or two solvation shells compared to unoriented solvent molecules. (2) A molecular-dipole-oriented geometry seems to be favored over a bond-dipole-oriented geometry, although no detailed studies of this particular question have been made. (3) The spin density on the first solvation shell protons is calculated to be negative.
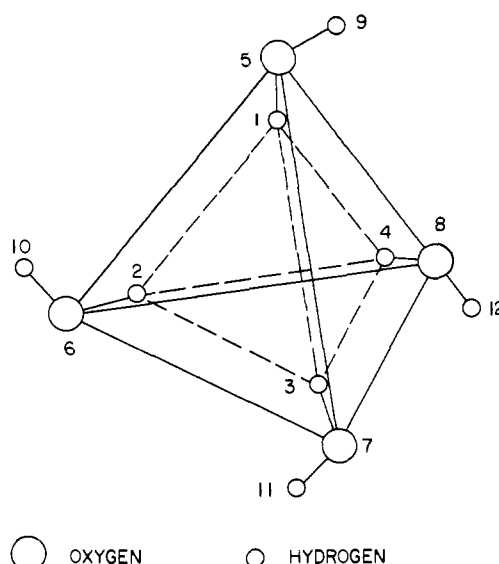

Figure 4. The tetrahedral molecular model for the hydrated electron as proposed by Natori and Watanabe.[26]

The disappointing aspect is that none of these results agree with experiment. It seems clear that long-range interactions must be included in some fashion. The one calculated feature that is at least consistent with experiment is the approximate size of the first solvation shell.

3. Molecular Field Model

Natori and Watanabe[28–30] have formulated a solvated electron model which is somewhat intermediate between a molecular orbital model and continuum models. They treat only short-range interactions, but they construct a potential from the wave functions of water molecules and treat the solvated electron independently of the electrons in the medium molecules. Thus they reduce a many-electron problem to a one-electron problem, as is done in continuum and semicontinuum models. The three papers of Natori and Watanabe discuss the same basic model with increasing rigor. Thus, only the last paper will be discussed here.

The trapping site is assumed to be created by four tetrahedrally oriented OH-bond-directed water molecules (see Figure 4). Neglecting the 1s electrons on the oxygen atom, we assume the remaining eight electrons in a water molecule to be allocated in pairs to two sets of two equivalent orbitals, $\chi(l_1)$, $\chi(l_2)$ and $\chi(b_1)$, $\chi(b_2)$. $\chi(l_1)$ and $\chi(l_2)$ are equivalent and are used to locate the two lone pairs on oxygen. The other equivalent pair, $\chi(b_1)$ and $\chi(b_2)$, are bonding orbitals assumed to be directed along the O–H bonds. The orbital directional parameters for a water molecule are determined by matching the calculated dipole moment with the experimental gas phase value, which is 1.840 D. The trial wave function of the hydrated electron is then assumed to be a combination of the 1s and 2s orbitals on the inner hydrogens and the 2s and 2p orbitals on the oxygens which are orthogonalized with the four water molecular wave functions.

The potential function V that enters into the Schrödinger equation is constructed from the wave function of the water molecule and, due to the symmetry of the system, is spherically symmetric. Using ice data for the OH bond distance and HOH bond angle, a singlet ground-state E_a and a triply degenerate higher energy state are obtained by applying the variational principle. The difference in the two energy levels is used to compare with the experimental optical absorption energy of the hydrated electron. Several other icelike structures are also calculated. The energy levels, oscillator strength, and hyperfine splitting constant are shown in Table IV. As the table shows,

TABLE IV. Calculated Results of the Molecular Field Model[a] for the Hydrated Electron

water structure		calcd						obsd		
b(OH), Å	θ(HOH), deg	l,[d] Å	E_a, eV	E_t, eV	f	$h\nu$, eV	A, G	A, G	f^a	$h\nu$,[b] eV
1.10	109.5 (ice)[c]	2.76	−1.94	−0.05	1.98	1.89	3.05	5.6	0.65	1.72
1.08	115 ⎫ distorted	2.76	−1.41	−0.02	0.82	1.39	3.33			
1.10	116 ⎬ ice	2.76	−1.32	−0.05	0.83	1.28	2.94			
1.10	116 ⎪ structure	2.62	−1.83	−0.08	4.22	1.74	2.63			
1.10	116 ⎭	2.65	−1.73	−0.05	4.63	1.68	2.70			

[a] M. Natori and T. Watanabe; see ref 28–30. The results in this table are obtained from ref 30. [b] See ref 30. [c] L. Pauling, "The Nature of Chemical Bond", 3rd ed., Cornell University Press, 1960, p 466. [d] One-half the diagonal distance between opposite corners of a tetrahedron.

there is no unique geometry of the trapping sites which can account for the observed values, although the calculated values are of the correct order of magnitude. Consequently, the results show that the interactions between the electron and the first solvation shell molecules are insufficient to account fully for what is observed. This point is consistent with the pure molecular orbital results.

4. Continuum Model

In the molecular field model[28-30] the excess electron is assumed to be under the influence of a fixed number of surrounding solvent molecules. In the continuum model this influence is extended to cover the entire medium, and the solvent molecules are only treated in an averaged manner. Consequently, the most striking difference between these two models is in the manner in which the trapping potentials are constructed.

In the molecular field model the potential only includes short-range interactions between the electron and the nearest four water molecules. These molecules can be viewed as forming the first solvation shell around the electron. All other interactions are assumed to be small and are neglected. In contrast, the continuum model makes no distinction between the nearest or further solvent molecules. The medium as a whole is represented by a continuous dielectric which is characterized by the macroscopic optical dielectric constant D_{op} and static dielectric constant D_s. When an electron is present at some point in the dielectric medium, the assumption is made that it will polarize its surroundings. The net effect of this polarization is the creation of a screened Coulomb potential well in which the electron can be trapped. This is the idea of self-trapping and was first introduced by Landau.[31] As will be seen later, the main advantage the continuum model has over all other models is its ability to handle a wide range of solvent media. Early application of the self-trapping concept resulted in a problem similar to a particle in a spherical box.

Jortner put electron binding in polar media on a sound theoretical basis. Combining the classical electrostatic idea on polarization with quantum mechanical methods and concepts, Jortner formulated the continuum model.[9a] In this model, the medium is assumed to be a polarizable continuous dielectric which is represented by static and optical dielectric constants. The electron is assumed to be located in a physical cavity which is spherically symmetric. At long distance the electron interacts with the continuous dielectric through a $1/r$ Coulombic potential while within and at the cavity boundary R the potential remains constant. This potential is assumed to be set up through the polarization of the medium, induced by the presence of the electron. The reference level for this potential is therefore the polarized medium.

To reduce an N-electron system to an effective one-electron problem, two approximations have been used: (1) adiabatic separation of the motion of the excess electron and the medium electrons and (2) assumption that the electron is moving in an average field created by the medium molecules. This latter approximation is the self-consistant-field method.

4.1. Adiabatic Approximation

In practice the two models differ in the form of the potential. Using the adiabatic approximation the potential takes the form

$$V(R) = -(D_{op}^{-1} - D_s^{-1})e^2/R, \quad r \geq R$$
$$V(r) = -(D_{op}^{-1} - D_s^{-1})e^2/r, \quad r \leq R \tag{1}$$

where R is the average cavity radius determined in this model by matching the calculated 1s → 2p transition energy with the experimental optical transition energy at the absorption maximum. The term $(D_{op}^{-1} - D_s^{-1})$ indicates that the trapping potential in this approximation derives only from the orientational polarization which cannot follow the motion of the excess electron and therefore is not state dependent. The energy of the excess electron due to orientational polarization is obtained by substituting the above potential in the Schrödinger equation and solving it variationally. The energy resulting from the electronic polarization S_i is calculated separately. The sum of these two energies gives the total energy of the ground state.

4.2. SCF Approximation

Rather than being considered separately, in the SCF approximation the orientational and electronic polarization are included simultaneously in the potential.

An electrostatic potential, f_i, that is consistent with the charge distribution of the electron, Ψ^2, is conveniently represented by Poisson's equation

$$\nabla^2 f_i = 4\pi e|\Psi_i|^2 \tag{2}$$

where f depends on the ith electronic state of the excess electron.

The potential energy $V(r)$ is now proportional to $(1 - D_s^{-1})$, which is related to both the orientational and electronic polarization (eq 3).

$$V(R) = (e/2)(1 - 1/D_s)f(R), \quad r \leq R$$
$$V(r) = (e/2)(1 - 1/D_s)f(r), \quad r \geq R \tag{3}$$

The notations used in eq 3 have the same meaning as in the adiabatic approximation. The solution of the one-electron Schrödinger equation using this potential and hydrogenic wave functions gives the total energy of the excess electron in the ground state.

4.3. Energy Level Calculation

The excited-state calculations in both the adiabatic and SCF approximations are very similar. In both it is assumed that the lowest optically allowed excited state is the 2p state. The energy of this state must be calculated in accordance with the Franck–Condon principle. That is, during vertical electronic transitions, the medium nuclei should be assumed fixed, so in the excited state the orientational polarization component is the

same as that in the state from which the transition originates. However, the electronic polarization follows the excitation process.

It is well-known that the energy of a particle in a box is inversely proportional to the box dimension. Similarly, the energy calculated from the adiabatic or SCF approximation decreases in absolute value with increasing cavity radius R. The R where the calculated $h\nu$ just matches the experimental value is assigned as R_0, so $h\nu$ is given by (4). In principle it is always

$$h\nu = E_t^{2p}(R_0) - E_t^{1s}(R_0) \qquad (4)$$

possible to get such a fit unless the experimental energy is greater than that calculated for $R = 0$.

Computations involved in the continuum model are extremely simple since the model is medium dependent only through the dielectric constants D_s and D_{op}. It can be readily applied to electrons trapped in a variety of media, both in liquids and glasses. Also, since the temperature dependence of dielectric constants is generally known, the shift of the optical absorption band as a function of temperature can be predicted. Calculations have been reported within the framework of the adiabatic approximation for electrons in liquid ammonia,[9c] MTHF glass,[32] and several other glasses.[33] Within the SCF approximation calculated results have been reported for liquid water.[9b,34]

Typically, the radius which yields agreement between the calculated and observed $h\nu$ for most systems appears to be quite reasonable. For example, the value of $R = 3.2$ Å for liquid ammonia is consistent with the large observed volume expansion data for that system compared with liquid ammonia. Also, the blue shift of the absorption band with decreasing temperature is consistent with shrinkage of the cavity.[9c] A real test of the continuum model is to compare the predicted and observed photoionization thresholds after the bound–bound optical transition energy has been fit to the experimental value by varying the cavity radius. Results on trapped electrons in MTHF glass[32] appear to meet this test reasonably well, but the results should be reevaluated with the proper value of D_s. In more polar matrices such as alcohols[33] and ice[11,34] the continuum model fails because it predicts photoionization thresholds which are greatly in excess of those observed experimentally. In addition, for solvated electrons in water the continuum model implies that the cavity radius is zero,[9] which is physically unreasonable.

Most of the published results using the continuum model have used a one-term, exponential "hydrogenic" wave function. If the trapping potential at or very near the cavity center still has the form of $-r^{-1}$, then the potential is very similar to the hydrogen atom situation and hydrogenic wave functions are suitable. However, this is not the case for the continuum model for a finite cavity radius. Thus, the question of whether a one-parameter hydrogenic wave function is still valid arises. Webster and Carmichael[35] recently investigated this problem by substituting the adiabatic and SCF potentials into the effective one-electron Schrödinger equation and solving it numerically. An examination of the radial charge density of the solvated electron in liquid ammonia and water indicates that the one-parameter wave functions[9b,c,34] generally yield higher average radii and a greater difference in shape for the ground state than for the excited state. Thus, the interpretation of calculated results based on trial wave functions should be done with caution particularly in regard to such properties as oscillator strength and line shape which are sensitive to the "correctness" of the wave function. The effect on energy levels and thus the optical transition energy is probably less sensitively dependent on the wave function, especially for these polar systems where the electrons are bound tightly in the cavity. When the one-parameter hydrogenic wave function gives particularly poor results as for the solvated electron in water,[9] a more flexible wave function may improve the situation. For example, a three-parameter wave function for the

solvated electron in water can fit the optical absorption energy at a finite cavity radius.[34]

The basic shortcoming of the continuum model is that no configurational stability is achieved. Furthermore the model lacks predictive power because usually one experimental observable like the optical absorption maximum is fit by one parameter in the wave function. These shortcomings can be overcome by explicitly treating short-range interactions with an oriented first solvation shell. This is done in the semicontinuum model.

5. Dipole Orientation Model

Before we discuss the semicontinuum model, we will describe Iguchi's[36,37] oriented-dipole model. The purpose of his study was to investigate the temperature dependence of the solvated electron optical maximum in alcohols. In his model the solvated electron is assumed to be surrounded by a number of dipoles n_m. This number is determined by the temperature of the system relative to $T_0 = 273$ K by eq 5, where a is the thermal expansion

$$n_m = \frac{n_0}{1 + a(T - T_0)} \qquad (5)$$

coefficient and has the value 1.0×10^{-3} K^{-1} for ethanol, and n_0 is the number density which equals 1.0×10^{22} cm^{-3} for ethanol. Since the denominator of (5) is 1, $n_m = 10^{22}$ cm^{-3}. Thus this model is essentially a molecular picture of the continuum model in which the partial orientation of all the dipoles is given by a Boltzmann distribution.

The potential energy used by Iguchi is given by eq 6, where

$$U(r) = -4\pi e\mu_0 n_m \int_r^\infty \langle \cos\theta \rangle dr \qquad (6)$$

$\langle \cos\theta \rangle = \coth\chi - \chi^{-1}$, $\chi = (\mu_0/kT)E_{loc}$, $E_{loc} = e/r_2$, μ_0 is the permanent dipole moment, and E_{loc} is the local electric field at the dipole due to the excess electron. Since the local electric field is independent of the charge density of the excess electron, unit charge density is included within radius r. Since the potential is independent of the solvated electron charge density, it is the same regardless of the electronic state. Upon evaluation Iguchi showed that the potential is long range, similar to the continuum potential.

For the medium rearrangement energy Iguchi calculated the dipole–dipole repulsion. In his model the number of dipoles that are around the electron is thermally determined and is on the order of 10^{22} cm^{-3}. Taking the electron as the coordinate center, dipole–dipole repulsions are cancelled out due to thermal fluctuations, and only dipoles within the first shell contribute to the localization of the electron.

In Iguchi's first paper[36] the potential shown in eq 6 was assumed to extend to the origin ($r = 0$). However, in the second paper[37] the potential was taken to be constant within a radius R, which was set equal to the average intermolecular distance. The energy due to orientational polarization, W_i, is calculated as in the continuum model with the adiabatic approximation. The electronic polarization energy, S_i, is calculated separately and added to W_i to give the total energy. Although Iguchi uses the same notation for energies as in the continuum model, it should be noted that they are calculated with a different potential.

In summary, Iguchi's oriented dipole model differs from the continuum model in that the former represents the polarizable medium by dielectric constants. The potential existing between the electron and the dipoles is short range (that is, dependent on r^n where $n \geq 2$) and temperature dependent. Long-range Coulombic interactions with potential dependent on r^{-1} are neglected. The potential used in the continuum model is temperature independent except through the temperature dependence of the dielectric constants, and only long-range interactions are included.
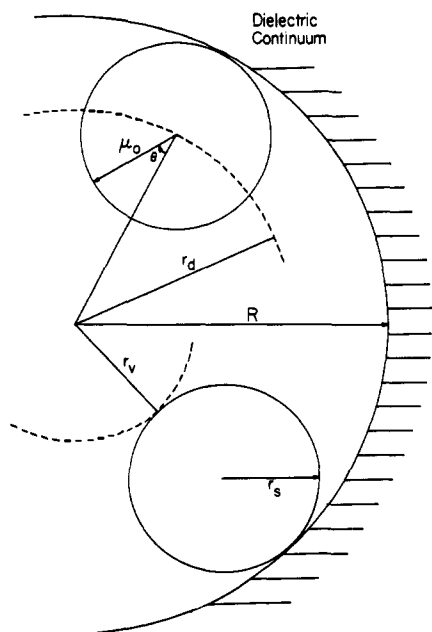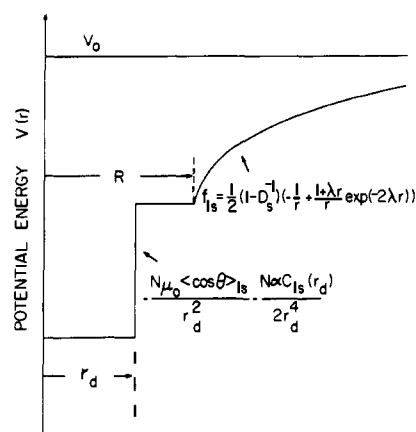
Figure 5. Distance parameters used in the FFK semicontinuum model for the solvated electron. The sum of the molecular radius r_s and the void radius r_v equals the electron to point dipole distance r_d. R is the distance to the beginning of the continuum.

Figure 6. Short-range well-type and long-range Coulombic potentials used in the FFK semicontinuum model. The energy reference level is the quasi-free-electron energy V_0. λ is a variational parameter in the wave function, D_s is the static dielectric constant, μ_0 is the dipole moment oriented at angle θ, α is the molecular polarizability, C_{1s} is the charge enclosed within the point dipole distance r_d, and N is the number of first solvation shell molecules.

6. Semicontinuum Model

6.1. Outline of Model

In the early development of the semicontinuum model Copeland et al.[10] and Fueki et al.[11] included both short- and long-range interactions between the solvated electron and the solvent or matrix molecules. A principal conclusion from those studies was that short-range attractive interactions must be included to properly account for the absolute value of the electronic energy levels. More specifically the inclusion of a short-range charge–dipole potential tends to move the energy levels toward the continuum, thus making the excited states less strongly bound. Satisfactory agreement between the calculated and experimental properties of the hydrated electron was obtained by arbitrarily choosing a cavity radius that gave the best fit with the experimentally measured optical absorption maximum. Clearly a more desirable approach is to minimize the total energy of the solvated electron system with respect to some coordinate in the same spirit as for a diatomic molecular system. This way the configuration of the trapping system can be predicted.

Two formulations of the improved semicontinuum model have been proposed.[10,38,39] Both of them originated from Jortner's continuum model.[9a] The physical ideas are very similar, and differences can only be found in the details of the calculations. The first model is the Copeland, Kestner, and Jortner (CKJ) model[10] where they assumed that the average velocity of the solvated electron is slower than the electrons of the solvent molecules. Consequently the trapping potential varies only as a function of solvent molecule–electron separation distance and not with the charge distribution of the electron. This is the so-called adiabatic approximation. On the other hand Fueki, Feng, and Kevan (FFK)[38,39] utilized the self-consistent-field approximation which implies that the solvent electrons and the excess electrons are basically equivalent and the solvated electron is under the influence of the averaged potential field generated by all other electrons. However, the potential is in turn modified by the presence of the excess electron. The CKJ model has been discussed in detail elsewhere[39] and therefore will not be reiterated here. The main differences between the two models will be pointed out later. The FFK model will be

discussed briefly to show the formulation of the model.

The semicontinuum model[39] differs from the continuum model[9a] in that the excess electron is assumed to be a charge distribution located at the center of a spherical cavity. The distance parameters are shown in Figure 5. Surrounding the cavity is a fixed number N of symmetrically situated solvent molecules. These solvent molecules are approximated as idealized point dipoles. Consequently the interactions between the excess electron and these solvent molecules are described by the standard charge–dipole attractive potential. As will be seen later, the charge distribution of the excess electron extends well into the first solvation shell; thus the polarization of these solvent molecules by the electron is expected to play some part in the localization of the electron.

Both of these interactions constitute a finite square well potential due to the fact that the potential is assumed to be invariant when the electron is inside the cavity. This electronic short-range potential is denoted by E_e^s. The solvent molecules beyond the first solvation shell are treated in a similar manner as in the continuum model:[9a,b] namely, in this region the electron interacts with the solvent molecules through a screened Coulombic long-range polarization potential denoted by E_e^l that is made self-consistent with the excess electron charge distribution via Poisson's equation. These long- and short-range interactions are the two leading terms in this model for the electronic component of the total energy. Figure 6 shows the total potential used in the FFK model.

The repulsion between the excess electron and the medium molecule electrons is approximated by $E_q = V_0(1 - C_i(r_d))$, where V_0 is the quasi-free-electron energy and $C_i(r_d)$ is the charge density for the ith state enclosed within radius r_d. For rare gas systems Springett, Jortner, and Cohen[40] have shown that V_0 can be calculated from the Wigner–Seitz model in which each atom is replaced by a sphere so that a spherical symmetric pseudopotential can be obtained. This pseudopotential is substituted into an eigenvalue equation whose solution is V_0. They showed that this term can be split up into two components, U_p and T_p, where U_p represents the attractive component due to long-range electronic polarization and T_p is the short-range repulsive scattering energy between the excess electron and the medium. By use of gas-phase scattering cross sections the results agree with experimentally measured V_0 values for rare gas systems and appear to correlate with electron mobility data.[41] Such a model has also shown to be valid for the temperature dependence of V_0 in liquid alkanes.[42,43] Due to the lack of accurate electron scattering data, V_0 for electrons in

TABLE V. Properties of Solvated Electrons in Polar Matrices Calculated by the Semicontinuum Model

Matrix	T, K	V_0, eV	N	$r_d{}^0$, Å	$h\nu$, eV calcd	$h\nu$, eV obsd	f calcd	f obsd	I, eV calcd	I, eV obsd	ΔH, eV	θ, deg
water	298	−1.0	4	1.93	2.15	1.72[a]	0.70	0.71[a]	3.63		2.75	14.1
			6	2.46	1.94		0.83		3.51		2.36	16.9
methanol	298	−0.2	4	2.28	1.85	1.87[b]	0.71	0.78[g]	3.23		2.09	16.6
			6	2.92	1.56		0.86		3.03		1.83	20.4
ethanol	298	0.2	4	2.54	1.79	1.80[b]	0.72	0.87[g]	3.10		1.77	17.9
			6	3.23	1.46		0.90		2.88		1.50	22.0
ice	77	−1.0	4	1.93	1.84	1.9[c]	0.39	0.33[h]	2.36	2.3 ± 0.1[c]	2.08	7.2
			6	2.46	1.85		0.64		2.45		1.72	8.6
methanol	77	0.5	4	2.32	2.09	2.3[d]	0.51	0.73[d]	2.73	2.4 ± 0.1[d]	1.33	8.3
			6	2.95	1.82		0.89		2.74		1.13	10.1
ethanol	77	1.0	4	2.54	2.15	2.3[d]	0.58	0.66[d]	2.71	2.4 ± 0.1[i]	1.02	10.0
			6	3.28	1.70		0.94		2.70		0.80	10.0
2-methyltetrahydrofuran	77	−0.5	4	2.87	1.04	1.0[e]	0.45	0.58[e]	1.42	1.6 ± 0.2[j]	1.35	10.3
			6	3.61	0.89		0.65		1.28		0.96	12.7
2-methyl-n-amylamine	77	0.3	4	3.24	1.02	1.1[f]	0.35		1.28	(1.2 ± 0.1)[k]	0.66	14.1
diisopropylamine	77	0.3	4	3.19	0.90	0.87[f]	0.36		1.16	1.0 ± 0.1[k]	0.57	16.0
triethylamine	77	0.3	4	3.19	0.83	0.75[f]	0.37		1.08	0.9 ± 0.1[k]	0.50	18.3
alkaline ice	77	0.0	4	2.04					1.04	1.5 ± 0.1[c]	0.30	7.4
			6	2.56					1.45		0.21	8.7

[a] E. J. Hart and M. Anbar, "The Hydrated Electron", Wiley-Interscience, New York, 1970. [b] M. G. Robinson, K. N. Jha, and G. R. Freeman, J. Chem. Phys., 55, 4974 (1971). [c] K. Kawabata, J. Chem. Phys., 55, 3672 (1971); L. Kevan, J. Phys. Chem., 76, 3830 (1972). [d] A. Habersbergerová, Lj. Josimović, and J. Teplý, Trans. Faraday Soc., 66, 656, 669 (1970). [e] T. Shida, J. Phys. Chem., 73, 4311 (1969). [f] S. Noda, K. Fueki, and Z. Kuri, Chem. Phys. Lett., 8, 407 (1971). [g] M. C. Sauer, Jr., S. Arai, and L. M. Dorfman, J. Chem. Phys., 42, 708 (1965). [h] G. Nilsson, H. Christensen, P. Pagsberg, and S. O. Nielsen, J. Phys. Chem., 76, 1000 (1972). [i] A. Bernas, D. Grand, and C. Chachaty, Chem. Commun., 1667 (1970). [j] T. Huang, I. Eisele, D. P. Lin and L. Kevan, J. Chem. Phys., 56, 4702 (1972). [k] S. Noda, K. Fueki, and Z. Kuri, Can. J. Chem., 50, 2699 (1972).

polar media cannot be evaluated theoretically. Also, V_0 in polar liquids cannot be measured directly by the usual photoelectric threshold experiments[43-46] because of high background currents. Very recent experiments show that V_0 can be measured indirectly in polar liquids,[47] but these data have not yet been used in semicontinuum model calculations. In any case V_0 can be reasonably estimated to be in the range −1 to +1 eV. So V_0 is treated as a limited adjustable parameter in the semicontinuum model. Note that the attainment of configurational stability is independent of the choice of V_0 since V_0 merely shifts the ground and excited energy levels.

To obtain configurational stability and therefore a uniquely determined cavity radius, appropriate work energy must be performed by the medium molecules for the formation of the cavity. To describe this situation the first shell dipole–dipole and induced-dipole–induced-dipole interactions are included as the short-range medium rearrangement energy, $E_m{}^s$. The long-range medium rearrangement energy involves the same polarization potential dependent on D_s and D_{op} as in the continuum model; it is denoted by $E_m{}^l$. At the boundary of the cavity, the energy is roughly approximated by the void energy E_v which depends on the surface tension of the medium. The sum of all these energy components together with the kinetic energy E_k of the electron yields the total energy of the system as given by eq

$$E_t(i) = E_k(i) + E_e{}^s(i) + E_m{}^s(i) + E_e{}^l(i) + E_m{}^l(i) + E_d(i) + E_v(i) \quad (7)$$

7 for the ith state. A one-parameter hydrogenic wave function is used in this energy expression with the variational method to obtain E_t as a function of r_d which gives a configurational coordinate diagram.

During an electronic transition the Franck–Condon principle must be obeyed. In the semicontinuum model this means that the orientational polarization potentials due to the first shell and the continuum are the same in the excited state as in the ground state. Only the electronic component of the polarization changes with the electronic state of the excess electron. Using the same concept, other states such as the relaxed 2p, 2s, and conduction states can be formulated easily. This provides a general outline

of the semicontinuum model. The explicit expressions used in the calculations for the ground, first excited, and other nonequilibrium states can be found in ref 12.

6.2. Applications of the Semicontinuum Model

6.2.1. Matrix Polarity

The attractive points of the semicontinuum model are as follows. (1) It seems to give the correct order of magnitude for the energy levels of the solvated electron. (2) For all the systems investigated a ground-state minimum energy is obtained along the configurational coordinate. This is the result of a delicate balance between negative electronic and positive medium rearrangement energies. (3) Most important of all the model can be used to investigate both polar and slightly polar systems with great ease.

The calculated results in general explain the experimental results due to changes in matrix polarity. For intermediate polarity systems such as the alcohols, the agreement is particularly good. The systems[12] that have been investigated by the above method are given in Tables V through VII along with the experimental results. The symbols in these tables are defined as follows. $r_d{}^0$ is the value of the electron to first solvation shell point dipole distance at the configurational minimum, $h\nu$ is the 1s → 2p bound–bound optical transition energy, f is the oscillator strength, I is the bound–continuum transition energy for the photoionization threshold, ΔH is the heat of solution which is the negative of the total ground-state energy at the configurational minimum, θ is the average point dipole orientation angle, and $C_i(r_j)$ is the charge density for electronic state i enclosed within a sphere of radius r_j. Figure 7 shows a typical configurational coordinate diagram, in this case for solvated electrons in an ether glass, methyltetrahydrofuran. In addition to the 1s, 2p, and conduction levels which are used in determining the properties tabulated in Tables V–VII, equilibrium 2s′ and 2p′ states are also shown in Figure 7.

Since the calculated properties of solvated electrons in different matrices are generally affected by several of the matrix properties summarized in Tables V–VII, it is not so simple to

TABLE VI. Charge Distributions of Solvated Electrons in Polar Matrices Calculated by the Semicontinuum Model

matrix	T, K	N	ground state			excited state		
			$C_{1s} (r_v°)$	$C_{1s} (r_d°)$	$C_{1s} (R_0)$	$C_{2p} (r_v°)$	$C_{2p} (r_d°)$	$C_{2p} (R_0)$
water	298	4	0.050	0.571	0.886	0.000	0.070	0.322
		6	0.174	0.646	0.893	0.011	0.198	0.529
methanol	298	4	0.076	0.631	0.913	0.001	0.100	0.396
		6	0.218	0.688	0.911	0.021	0.260	0.610
ethanol	298	4	0.083	0.675	0.935	0.001	0.134	0.482
		6	0.232	0.722	0.930	0.030	0.341	0.713
ice	77	4	0.048	0.563	0.881	0.000	0.018	0.118
		6	0.172	0.642	0.891	0.005	0.105	0.348
methanol	77	4	0.092	0.666	0.929	0.001	0.068	0.301
		6	0.250	0.726	0.929	0.037	0.361	0.727
ethanol	77	4	0.094	0.710	0.949	0.001	0.121	0.454
		6	0.273	0.764	0.947	0.060	0.487	0.838
2-methyltetrahydrofuran	77	4	0.083	0.650	0.922	0.000	0.036	0.191
		6	0.206	0.678	0.907	0.006	0.110	0.352
2-methyl-n-amylamine	77	4	0.052	0.702	0.954	0.000	0.036	0.214
diisopropylamine	77	4	0.042	0.683	0.949	0.000	0.028	0.183
triethylamine	77	4	0.040	0.671	0.945	0.000	0.026	0.172
alkaline ice	77	4	0.075	0.602	0.895	0.000	0.000	0.000
		6	0.217	0.684	0.909	0.000	0.000	0.000

TABLE VII. Various Energy Contributions to the Total Energy of Solvated Electrons in the Excited State Calculated by the Semicontinuum Model

matrix	T, K	N	E_k, eV	E_e^s, eV	E_m^s, eV	E_e^l, eV	E_m^l, eV	E_v, eV	E_q, eV	E_t, eV
water	298	4	1.208	−0.417	0.743	−3.066	1.762	0.099	−0.930	−0.601
		6	1.491	−1.110	1.204	−3.075	1.636	0.231	−0.802	−0.426
methanol	298	4	1.074	−0.405	0.442	−2.754	1.538	0.047	−0.180	−0.238
		6	1.307	−1.002	0.756	−2.696	1.410	0.106	−0.148	−0.266
ethanol	298	4	1.059	−0.460	0.380	−2.588	1.403	0.056	0.173	0.024
		6	1.350	−1.142	0.710	−2.510	1.289	0.126	0.132	0.045
ice	77	4	0.566	−0.566	0.698	−1.462	0.912	0.138	−0.982	−0.237
		6	0.963	−0.592	1.143	−1.772	0.962	0.320	−0.895	0.130
methanol	77	4	0.823	−0.269	0.406	−1.755	0.983	0.099	0.466	0.755
		6	1.705	−1.486	0.923	−2.013	1.024	0.218	0.320	0.690
ethanol	77	4	0.992	−0.425	0.386	−1.721	0.778	0.112	0.236	1.133
		6	1.873	−1.781	0.927	−1.801	0.795	0.263	0.513	0.900
2-methyltetrahydrofuran	77	4	0.370	−0.094	0.216	−1.109	0.623	0.166	−0.482	−0.309
		6	0.461	−0.284	0.389	−1.180	0.626	0.354	−0.445	−0.079
2-methyl-n-amylamine	77	4	0.290	−0.048	0.069	−0.864	0.468	0.150	0.289	0.354
diisopropylamine	77	4	0.263	−0.030	0.043	−0.828	0.453	0.138	0.292	0.331
triethylamine	77	4	0.252	−0.022	0.027	−0.812	0.446	0.138	0.292	0.332

describe separately the way that each of these properties affects the properties of the solvated electrons. Nevertheless, some general comments are extremely useful from an experimental point of view and are attempted here. The energies of solvated electrons are rather insensitive to values of the surface energy term and of D_{op} because they do not vary much between matrices. The energies are also largely insensitive to the effective molecular radius of the solvent molecules within a few tenths of an angstrom.

The permanent dipole moment of the matrix molecule contributes to the orientational polarization energy of the molecules in the first solvation shell. This orientational polarization energy increases in its magnitude with increase of the permanent dipole moment. This is seen when the properties of solvated electrons in glassy amines are compared to those in glassy methanol and ethanol. The permanent dipole moment also contributes to the short-range medium rearrangement energy by dipole–dipole repulsion between the oriented dipoles in the first solvation shell. This interaction partially cancels the short-range attractive interaction. The clearest effect of changing the dipole moment is illustrated by the amine results in which all matrix properties except the dipole moment and V_0 are the same. Both $h\nu$ and I increase with the dipole moment, but the fractional changes in $h\nu$ and I are smaller than those in the dipole moments. Also, the increased dipole moment stabilizes the ground state but destabilizes the first excited and continuum states. However, the effect on the ground state predominates. Among methanol, ethanol, and MTHF glasses, the dipole moment is not the con-
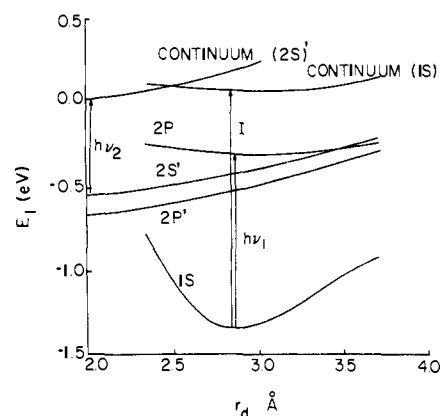
Figure 7. A typical configurational coordinate diagram calculated from the FFK semicontinuum model. This is the case of an electron trapped by four MTHF solvent molecules at 77 K. 1s is the ground-state energy; 2p and continuum(1s) refer to the nonequilibrium excited and conduction states respectively. 2s' and 2p' are the relaxed excited states. Continuum(2s') is the nonequilibrium conduction state.

trolling factor for determining $h\nu$ or I. Also V_0 is not taken to be the same for these matrices, and this obscures the relatively small effect of the dipole moment on the energy levels. The molecular polarizability of the matrix molecule contributes to the electronic polarization energy of the molecules in the first solvation shell. The polarizability is also related to the short-range medium rearrangement energy, since the polarizability is included

TABLE VIII. Pressure Effect on the Properties of the Solvated Electron in Methanol at T = 298 K Based on Semicontinuum Model Calculations

N	p, kbar	V_0, eV	$r_d{}^0$, Å	f	I, eV	ΔH, eV	θ, deg	$h\nu$(calcd), eV	$h\nu$(obsd),[a] eV
4	0.001	−0.2000	2.28	0.714	3.230	2.089	16.6	1.851	1.87
	1.50	−0.0885	2.24	0.690	3.287	1.895	16.2	1.945	1.91
	2.76	−0.0182	2.18	0.674	3.332	1.743	15.8	2.009	1.98
	4.14	0.0343	2.18	0.670	3.351	1.589	15.8	2.037	2.05
6	0.001	−0.2000	2.92	0.865	3.026	1.830	20.4	1.564	
	1.50	−0.0885	2.82	0.852	3.120	1.548	19.6	1.681	
	2.76	−0.0182	2.76	0.842	3.168	1.330	19.3	1.742	
	4.14	0.0343	2.71	0.832	3.204	1.109	18.9	1.791	

[a] M. G. Robinson and G. R. Freeman, private communication, 1971.

in the effective dipole moment as the induced dipole moment. So, increased polarizability is expected to have a similar effect to increased dipole moment, if all other matrix properties and V_0 are held constant. If the magnitude of the permanent dipole moment is about the same, there is an empirical, but not causative, trend between polarizability and V_0. This apparent trend can be seen for solvated electrons in liquds and for trapped electrons in ice, glassy methanol, and ethanol. Although MTHF has a rather large polarizability, it was necessary to assume a lower value of V_0 in MTHF than expected from the above trend to account for the low optical transition energy of trapped electrons in MTHF.

The static dielectric constant of the matrix contributes to the long-range orientational polarization energy of the continuous dielectric medium. But, the static dielectric constant at 77 K is very similar in the different glassy matrices, so it does not affect the energy levels strongly. However, D_s does dominate the effects on the electron energy levels in liquids compared to 77-K solids.

The energy of the continuum electron state, V_0, is largely due to a balance between polarization forces, which give a negative contribution, and electron–molecule repulsion, which gives a positive contribution.[10] An increase in V_0 in the same matrix increases $h\nu$ and decreases ΔH. The values of V_0 used to give fits to experimental $h\nu$ values do not appear to fit any general correlation with matrix properties.

We may consider the solid matrices to decrease in general polarity in the order methanol, ethanol, MTHF, 2-methylamylamine, diisopropylamine, and triethylamine. The values of $h\nu$ generally decrease with decreasing polarity. The value of I also generally decreases with polarity, but the quantity $I − h\nu$ is perhaps more significant. $I − h\nu$ represents the stabilization of the first excited state with respect to the conduction state, and this energy generally decreases with decreasing polarity; $I − h\nu$ averages 0.57 eV for alcohols, 0.38 eV for MTHF, and 0.26 eV for amine glasses.

The value of $r_d{}^0$ may be regarded as a rough measure of the size of the electron wave function. In recent electron–nuclear double resonance experiments,[48] the experimental values of the average size of the trapped electron wave function in several glassy matrices appear to be in approximate agreement with the $r_d{}^0$ values. The $r_d{}^0$ values increase with decreasing polarity, but this does not necessarily mean that the electron cavity size is increasing. Recall that $r_d{}^0 = r_s + r_v{}^0$, where r_s is the radius of the matrix molecule and r_v is the electron void radius. One finds that $r_v{}^0$ is reasonably constant for the matrices studied and equals 0.71 ± 0.06 Å.

6.2.2. Pressure Effects

Schindewolf et al.[49] found that the optical absorption bands of the electron in water and in ammonia shift to higher energies as the pressure is increased to 1 kbar. Similar results at several kilobars have been seen for the solvated electron in water[50] and in alcohols[51] by pulse radiolysis. Rather than empirically at-

tributing this to the contraction of the cavity radius, the semicontinuum model accounts for the pressure dependence with the following modifications. (1) At higher pressure the pressure–volume work becomes significant and is written as

$$E_{pv} = \tfrac{4}{3}\pi(R^3 - Nr_s{}^3)p \qquad (8)$$

(2) The pressure dependence of the optical dielectric constant is obtained via the density from the Clausius–Mossotti equation. (3) The V_0 value is also a function of pressure via its density dependence. The calculations appear to account for the experimental results for methanol and ethanol at room temperature. It appears that not only a decrease of the cavity radius but also an increase in the quasi-free-electron energy, V_0, are important in the interpretation of the spectral shift observation. The results are shown in Table VIII.

6.2.3. Temperature Effects

Decreasing the temperature causes the same spectral shift as increasing the pressure due to the density changes. The temperature parameter is built into the semicontinuum model explicitly through the Langevin function which determines the degree of dipole orientation at thermal equilibrium. Kestner, Jortner, and Gaathon[52] have shown that the temperature dependence of the spectral shift can not be explained by the Langevin factor and the temperature dependence of the static dielectric constant. However, Fueki, Feng, and Kevan[53] have shown that by the inclusion of the temperature dependence of V_0 and the dipole moment, a good correlation is obtained. These results are shown in Table IX.

6.2.4. Dipole Reorientation Effect

Hase et al.[54] have observed that when ethanol glass is irradiated at 4 K the trapped electron spectrum peaks in the IR region instead of in the visible region. However, upon warming the spectrum shifts irreversibly to the visible region. The 4 K results indicate that the electron is trapped in a nonequilibrium environment characterized by a shallow potential while at 77 K the electron is trapped in an equilibrium environment characterized by a deeper potential. Both nano- or picosecond time-scale pulse radiolysis and the effect of scavengers on the spectral shifts give strong experimental evidence that the electrons initially localized in shallow traps are not thermally excited out of these traps and ultimately redistributed in deeper traps but rather that the first solvation shell molecules reorient around the electron to generate a deeper potential.[1] To test this theoretically, calculations have been done within the framework of the semicontinuum model.[55] Explicitly the transition energy 1s → 2p is calculated as a function of the dipole orientation angle, θ. The nonoriented shallow trap is approximated by $\theta = 80°$ while the equilibrium orientation corresponds to $\theta = 0–10°$. The changes of the various energy levels as a function of the angle θ are shown in Figure 8. The observed shift is from 1500 (0.83 eV) to ~600 nm (2.1 eV) while the

TABLE IX. Temperature Effect on the Properties of the Solvated Electron in Methanol, Ethanol, and 1-Propanol for
N = 4 Based on Semicontinuum Model Calculations

T, K	$r_d{}^0$, Å	f	I, eV	ΔH, eV	θ_{th}, deg	$h\nu$(calcd), eV	$h\nu$(obsd),[a] eV
Methanol							
140	2.28	0.723	3.788	2.220	10.1	2.268	
160	2.28	0.720	3.751	2.230	10.9	2.243	
183	2.28	0.717	3.692	2.234	11.7	2.205	2.22
195	2.28	0.713	3.662	2.234	12.1	2.183	2.20
243	2.28	0.707	3.514	2.209	13.8	2.080	2.07
294	2.28	0.702	3.362	2.169	15.7	1.974	1.95
320	2.28	0.702	3.287	2.154	16.6	1.923	1.90
336	2.28	0.702	3.246	2.144	17.1	1.897	1.84
358	2.28	0.702	3.193	2.134	17.8	1.865	1.75
Ethanol							
140	2.56	0.805	3.708	1.845	11.1	2.201	
155	2.56	0.797	3.659	1.850	11.7	2.172	2.27
173	2.56	0.783	3.581	1.842	12.5	2.123	2.23
195	2.51	0.737	3.467	1.816	13.4	2.072	2.13
234	2.51	0.716	3.275	1.777	15.3	1.936	2.03
296	2.51	0.702	3.086	1.776	17.6	1.816	1.80
323	2.51	0.708	3.006	1.783	18.5	1.767	1.73
343	2.51	0.697	2.943	1.788	19.1	1.730	1.66
1-Propanol							
129	2.83	0.888	3.555	1.623	11.5	2.049	
147	2.83	0.868	3.480	1.628	12.3	2.015	2.25
173	2.77	0.816	3.363	1.616	13.5	1.978	
195	2.77	0.787	3.231	1.592	14.7	1.898	
227	2.77	0.755	3.081	1.576	16.3	1.805	
249	2.77	0.744	3.005	1.577	17.3	1.759	
273	2.77	0.731	2.929	1.584	18.2	1.713	
298	2.77	0.720	2.849	1.590	19.2	1.668	1.67[b]

[a] K. N. Jha, G. L. Bolton, and G. R. Freeman, *J. Phys. Chem.*, 76, 3876 (1972).   [b] M. C. Saurer, S. Arai, and L. M.
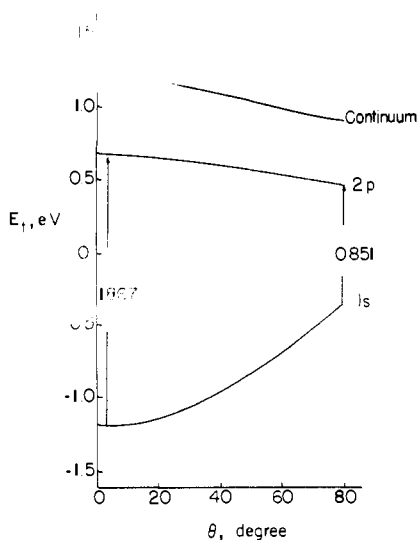Dorfman, *J. Chem. Phys.*, 42, 708 (1965).

Figure 8. Variation of the energy levels of the localized electron in ethanol glass at 77 K with the angle of dipole orientation θ for four ethanol molecules in the first solvation shell and a quasi-free-electron state energy of 0.5 eV at radii corresponding to the configurational minimum energy of the ground state.[55]

Figure 9. Distance parameters used in the CKJ semicontinuum model for the solvated electron.[10] The definitions are the same as in Figure 5 with the addition of the hard-core molecular radius $\tilde{a}$.

calculated values are 0.85 eV (θ = 80°) and 1.87 eV (θ = 0°).

6.3. Comparisons of the CKJ and FFK Models

The Copeland, Kestner, and Jortner (CKJ) semicontinuum model uses the adiabatic approximation. Calculations with this model have focused mainly on the excess electron in dilute metal–ammonia solutions. Where comparisons can be made the general features of the calculated results from the CKJ and FFK models are similar. Nevertheless, it is useful to summarize the theoretical differences between these two models.
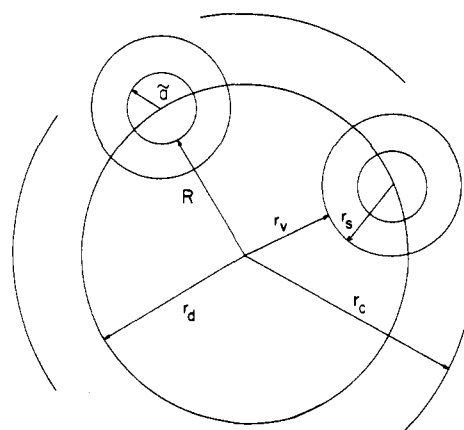
(1) Perhaps the most significant difference between the two models is in the long-range potential. The long-range potential in the FFK semicontinuum model is self-consistent with the charge density of the excess electron, and it is obtained from the solution of Poisson's equation. The energy level calculation in the CKJ model involves the adiabatic approximation; the long-range potential is therefore created by a point charge located at the center of the cavity. A comparison of the results calculated from these two models is given in Table X. It is clear that the differences are not large. Although the dielectron problem is not discussed in this review, it should be pointed out that the difference in the long-range potential treatment is magnified when two spin-paired electrons reside in a common cavity.

(2) In the distance definitions, the CKJ model introduces an additional parameter, namely the hard-core molecular radius $\tilde{a}$

TABLE X. Comparison of the CKJ and FFK Semicontinuum Models with Numerical Results on Solvated Electrons in Liquid Ammonia and Water

system	method	potential	r_d, Å	$h\nu(1s \rightarrow 2p)$, eV	ΔH, eV	V_0, eV
NH_3	variational[a]	adiabatic	2.75	1.03	0.909	0.0
	numerical[c]	adiabatic	2.70	1.237	1.051	0.0
	experimental			0.80	1.7 ± 0.7	
H_2O	variational[b]	SCF	1.93	2.15	2.75	-1.0
	numerical[c]	SCF	1.83	2.717	3.282	-1.0
	experimental			1.72	1.7	

[a] N. R. Kestner, "Electrons in Fluids", J. Jortner and N. R. Kestner, Ed., Springer, Berlin, 1972. Here a more refined short-range molecular potential is used than in the original CKJ model. [b] K. Fueki, D. F. Feng, and L. Kevan, J. Am. Chem. Soc., 95, 1398 (1973). [c] B. C. Webster and I. Carmichael, J. Chem. Phys., 68, 3086 (1978).
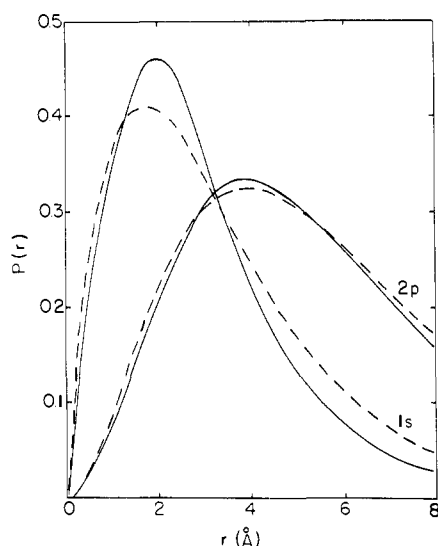

Figure 10. Comparisons of the ground 1s state and excited 2p wave functions for the ammoniated electron as determined by the CKJ semicontinuum model using the variational method (broken curve) and the numerical method (solid curve).[56]
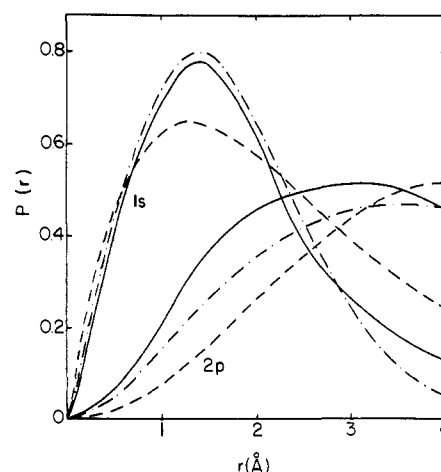

Figure 11. Comparisons of the ground 1s state and excited 2p state wave functions for the hydrated electron as determined by the FFK model using the numerical (solid curve) and variational methods (----, hydrogenic wave functions; ----, Guassian wave function).[56]

(see Figure 9). This is approximated from theoretical charge contour data and in effect $\tilde{a}$ prevents the excess electron from coming too close to the solvent molecules in the first solvation shell. There is no corresponding parameter in the FFK semicontinuum model. However, Copeland et al.[10] have shown that very little difference results by including this parameter.

(3) Because the CKJ model uses the adiabatic approximation and the FFK model employs the self-consistent-field approximation, the method for energy evaluation in the two models is different. Rather than applying the variational principle to the total energy (electronic plus medium rearrangement energy) as is done in the FFK model, in the CKJ model it is applied only to the electronic energy. The parameters determined from the electronic energy calculation are subsequently used for calculating the medium rearrangement energy E_m. The sum of the two constitutes the total energy of the system. Although the two models yield similar total energies (see Table X) for the liquid ammonia case, only the FFK semicontinuum model attains configurational stability for the aqueous system.

(4) In the CKJ model an estimated hydrogen–hydrogen repulsion energy is included in the total energy of the system.

6.4. Numerical Evaluation of the Semicontinuum Model

Webster and Carmichael used the semicontinuum potential in both the adiabatic and SCF approximations and solved the Schrödinger equation by using numerical integration.[56] It is interesting to compare the wave function in terms of charge density obtained from the numerical method and the variational procedure. Figure 10 shows the ground and first excited 2p

charge density of the ammoniated electron using the adiabatic approximation. Figure 11 shows the corresponding plots calculated within the SCF approximation. It is clear from the figures that both the 1s and 2p hydrogenic wave functions assumed for the excess electron deviate considerably from the numerical results. With a Gaussian wave function,[57] the ground state matches well with the numerical results at and around the maximum charge density; but at large distances from the electron in the ground state and at all distances in the excited state, the agreement is poor. Of course, we must remember that the results calculated using the numerical methods do not necessarily imply that better agreement with experiment should be attained. In fact, the agreement is not as good as with the variational calculation. This is due to the fact that the numerical results still hinge on the "correctness" of the guessed trapping potential.

As expected, the total energy obtained by numerical integration as a function of the configurational coordinate is lower than that obtained from the variational procedure. The difference is greater for the ground state than for the first excited state. Table X summarizes these comparisons. Due to the differences in the ground-state energy the physical properties predicted from the numerical method such as $h\nu(1s \rightarrow 2p)$ and ΔH are greater than those calculated using the variational principle.

Webster and Carmichael suggest that the polarizability of the solvated electron may serve as a good test of the theoretical model. The polarizability can, in principle, be calculated from a moment theory analysis of the optical absorption spectrum independent of any particular molecular model. However, such a determination depends critically on the accuracy with which the tails of the optical absorption are known. From the available data the polarizabilities of the solvated electron in liquid ammonia and water are estimated to be 113.4 and 26.6 Å³, respectively.[56]

TABLE XI. Newton's "ab Initio" Semicontinuum Model for the Hydrated and Ammoniated Electrons[5]

calculated results	U^a	solvent molecules S				
		hydrated electron			ammoniated electron	
		I^b	II^d	IIIe	I^b	IIe
$E(S)_4^- - E(4S)$, eV	0	0.34				
		−0.88				
$E(S)_4^- - E(S)_4$, eV	0	−0.06				
		−1.62				
$r_d^{\,0}$, Å		2.65^c	2.5	1.93	2.75^c	3.0
$C(R)$, ground state	0	0.72				
		0.84		0.886	0.43	0.210
hv, eV		1.20		2.15	0.50	1.72
ΔH, eV		2.15		2.75	1.51	2.45
e_H^{spin}, Å^{-3}		−2.9 × 10^{-3}			−0.63 × 10^{-3}	
a_H, G		−4.6			−1.0	

^{a} U is the polarization energy. When $U = 0$ it means that the dielectric continuum is neglected in the calculation. When U is included in the variational calculation, the U value is omitted from the table. ^{b} Results taken from ref 5. All results are calculated based on $V_0 = 0$ eV. The hydrated electron results are calculated for 298 K while the ammoniated electron is calculated for 240 K. ^{c} The variationally calculated cavity radius, $r_d^{\,0}$, is slightly larger than this value. This value is obtained by taking into account the hydrogen-bonding effect, temperature effect, etc. ^{d} See ref 22. The 2.5-Å value for $r_d^{\,0}$ is selected for comparison only. It is not a result that comes from the variational calculation of the total energy. ^{e} Semicontinuum model results for the hydrated electron are from ref 58 and for the ammoniated system from ref 10.

These values are bracketed by the continuum and the semicontinuum potential results.

6.5. Newton's "ab Initio" Semicontinuum Model

As a result of the extensive studies based on the semicontinuum model the following facts seem clear for solvated electrons in polar media. (1) To account for the unusual stability of the electron in condensed phases detailed interactions between the electron and its immediate neighbors must be included. (2) These short-range interactions are not solely responsible for the solvation process; the bulk medium also plays a major role in keeping the electron localized in a cavity. (3) To obtain a meaningful configurational stability of the excess electron the medium rearrangement energy must be included to compensate for the strong electron–medium interactions.

In the semicontinuum model the short-range interactions are treated by a classical potential. A better representation of the interaction of the electron with the first solvation shell molecules can be achieved by ab initio methods as discussed in section 2. However, the long-range interactions must also be included, and for them it seems most tractable to retain the classical polarization treatment used in the semicontinuum model. The question is how to combine the usual ab initio molecular orbital formalism with the classical electrostatic polarization treatment so that the electron and its immediate neighbors can be included explicitly while the bulk of the solvent molecules can be considered as a continuum characterized by such macroscopic parameters as the static and optical dielectric constants.

Newton[5] devised a method to link the ab initio MO method with an excess electron imbedded in a polarizable continuum and has provided the most complete calculations on the hydrated and ammoniated electron systems to date. In his model the electron is assumed to be at the center of a spherical cavity composed of four solvent molecules arranged tetrahedrally. The model assumes that in a symmetrical system the total energy of an excess electron in its ground state is expressed by

$$E = E^\circ + \tfrac{1}{2}(1 - 1/D_s) \int_0^\infty d\tau d\tau' \rho(r)g(r,r')\rho(r') \quad (9)$$

E° is the usual unrestricted Hartree–Fock energy which takes into account the interactions between the excess electron and the nearest solvent electrons and also the interactions among the electrons of the solvent molecules. This replaces the short-range charge–dipole and dipole–dipole repulsion terms in the FFK semicontinuum model. The second term in (9) corre-

sponds to the energy of the medium beyond the first solvation shell as it is polarized by the charge density $\rho(r)$ of the electron. The bulk medium is treated as a continuum as in the FFK semicontinuum model and is characterized by the static dielectric constant D_s. This part of the energy can be "switched off" to examine the effect of the immediate neighbors on the stabilization of the excess electron in the cavity. To further generalize the equation, Newton added energy E_q to the total energy. This term approximates the repulsive interactions between the excess electron and the bulk solvent electrons. This term is only significant when the electron extends well beyond the first solvation shell.

It is found that it is slightly more favorable for the molecular dipole of the solvent to be approximately oriented toward the center of the cavity than for the OH or NH bonds to be so oriented. However the energy difference between dipole-oriented or bond-oriented configurations is within the calculational uncertainty. For the hydrated electron case Newton also investigated a pentamer model in which one additional water molecule is placed at the center of the cavity with all the water molecules in an icelike structural configuration. Again the above dipole-oriented tetramer is slightly more stable.

Some of the calculated results are listed in Table XI. Some FFK and CKJ semicontinuum model results are also included for comparison.

As mentioned earlier, one of the advantages of using the molecular orbital method is that it can give some information as to how stable the cavity system is with respect to $E(4S)$ or $E(S)_4$. Based on the second and third row results in Table XI it can be seen that the solvated electron system is unstable with respect to four isolated molecules, particularly if the dielectric continuum is neglected. However, when the continuum is included, the solvated electron is strongly bound relative to four tetrahedrally oriented neutral molecules. This, coupled with the charge distribution, $C(R)$, strongly supports the idea that (1) second or higher solvation shells are necessary for localization of the electron and (2) the relative energies provide a rough picture of what type of energy magnitudes are involved during the solvation process. The model provides good agreement between the calculated and experimental values of the optical absorption maximum for both the hydrated and ammoniated electron systems. This however requires limited adjustment of the quasi free electron energy, V_0, to be 1 eV. The signs of the calculated spin density on the protons are negative for both systems. For the ammoniated system this may be consistent with experimental Knight shift data; however, the experimental

conclusions are not unambiguous. In the hydrated electron case, however, electron spin–echo data seem inconsistent with a negative spin density on the protons.[27] Further theoretical and experimental work on the spin density sign inconsistency is desirable.

Newton's calculations clearly support the semicontinuum model results that the electronic wave function extends well into the dielectric continuum and that the localization process must involve solvent molecules beyond the first solvation shell.

6.6. Semicontinuum Model for Nonpolar Media

It has been well documented[1] that electrons generated by γ irradiation or photoionization of a suitable solute can be localized and solvated in both polar and nonpolar media. In polar media the electron is localized due to the strong interactions between the electron and the dipole moment of the solvent molecules. This is the cavity model, and it is generally well accepted. In nonpolar media the molecular dipole moment and the difference between the optical and static dielectric constants are essentially negligible. Furthermore, since the excess electrons in nonpolar media all absorb light at about the same wavelength (1700–2000 nm), the formulation of a theoretical model based on the extension of the semicontinuum model to nonpolar systems become less obvious. However, Magat[58] has given some qualitative energetic arguments as to why electrons can be trapped in nonpolar media. These were based on a modified "bubble" model which has worked well for rare gas systems.

The development of the semicontinuum model to electrons in nonpolar media was based on a number of experimental data relating to such systems. For instance, recent electron spin–echo studies on solvated electrons in 3-methylpentane glass suggest that there are 18–20 equivalent nearest protons approximately 3.0 Å away from the solvated electron.[59] The possibility that C–H bond dipoles may play a role in the solvation process is indirectly reflected from pulse radiolysis results on the time to reach stable optical spectra as a function of matrix polarity.[1] The conduction electron energy V_0 provides information on the electron–medium interaction when the electron is mobile or in a delocalized conduction state relative to the vacuum state. For polar systems this parameter has been argued on theoretical bases to be small and in the range −1 to +1 eV. However, now a number of V_0 values have been measured using a photoionization threshold method for a variety of alkanes.[43-45] These values can be used directly in the semicontinuum model when it is properly modified for nonpolar systems. The mobilities of excess or quasi-free electrons in the delocalized conduction state also provide relevant dynamic information about the electron. However, the large range of electron mobilities over three orders of magnitude[60] suggests that the geometrical structure of the solvent molecules around the electron can have important energy effects.

Since semiquantitative understanding of electrons in polar solvents seems to have been achieved by the semicontinuum model,[12] Feng, Kevan, and Yoshida[61] first examined the possibility of electron localization in alkanes via CH bond dipoles. This model, which can be called the FKY microdipole model, assumes that the electron resides in a spherical cavity constructed from N symmetrically oriented CH_2 fragments. In the calculations $N = 4$, 8, and 12 were considered. The various energy terms take the same form as for polar media with the dipole moment and polarizability being replaced by the CH bond dipole and CH_2 fragment polarizability evaluated from the parallel and perpendicular components. The only other term that is clearly different from polar media is the dipole–dipole repulsion term. The repulsions between finite CH bond dipoles are represented by eq 10, where k and l refer to a pair of finite dipoles whose magnitudes are $|\vec{m}_k|$ and $|\vec{m}_l|$ separated by a distance $|\vec{r}_{kl}|$. For the

$$E_m{}^s(i) = \frac{\vec{m}_k \cdot \vec{m}_l}{|\vec{r}_{kl}|^3} - 3\frac{(\vec{m}_k \cdot \vec{r}_{kl})(\vec{m}_k \cdot \vec{r}_{kl})}{|\vec{r}_{kl}|^5} \tag{10}$$

m's, both the permanent and the induced dipole moments are included. Although V_0 values have been measured for many nonpolar media, in this calculation values of 0.5, 0, −0.5 eV are used to examine the sensitivity of the calculated results to this parameter. The total energy of the electron in the ith state (eq 11) is calculated in the same manner as for polar systems using

$$E_t(i) = E_k(i) + E_e{}^s(i) + E_m{}^s(i) + E_e{}^l(i) + E_m{}^l(i) + E_q(i) + E_v \tag{11}$$

the variational principle. Energy values obtained at various r_d values are then used to construct the configurational coordinate diagram.

In addition to examining the dependence on V_0 and on the number of solvent molecules around the solvated electron, other parameters were also varied. For example, distortion of the HCH bond angle away from the regular tetrahedral value and decreasing the bond dipole value by a factor of two were investigated and found to have only a minor influence on the results. The 1s → 2p transition energy $h\nu$ increases with V_0. This is in the same direction, although with a lesser change in magnitude, as that found in polar solvents. When N is increased from 4 to 12, the stability factor, $V_0 - E_t$ (1s), defined by Fueki and Kevan, drops from approximately 0.3 to 0.03. This is inconsistent with later spin–echo results[59] which suggests $N \sim$ 9.

In comparison with polar systems, all the different N cases calculated are very weakly stable or unstable. This is due to an overestimation of the dipole–dipole repulsion term given by eq 10. The case for $N = 4$ gives the most favorable calculated optical absorption energy. The results of this calculation are listed in Table XII for comparison with other models. As one can see, the calculated 1s → 2p transition energy is only slightly greater than half of the observed value.

Nishida developed a modification of the FKY microdipole model for electrons in nonpolar solvents. He assumed that the CH bond microdipoles could be neglected on the basis that the electron–microdipole attractive interaction was approximately canceled by the microdipole–microdipole repulsive energy. Kimura et al.[63] simultaneously suggested the same approximation reasoning from new experimental data (see below). Nishida also assumed that each molecule could be represented by a CH fragment and that the exchange interaction between the carbon core and the excess electron was large enough to be explicitly included. For N CH fragments the induced dipole interaction energy is

$$E_e{}^s(i) = -\int_{r \le r_d} \Psi_i \frac{Ne^2\alpha C_i}{2r_d{}^4} \Psi_i d\tau \tag{12}$$

where α is the polarizability of the CH bond, r_d is the distance from the cavity center to the carbon atom (see Figure 10), Ψ_i is the excess electronic wave function in state i, and C_i is the charge distribution within r_d. This is the same equation as in the FKY microdipole model with $\mu(CH) = 0$. By assuming $\mu(CH) = 0$ the short-range medium rearrangement energy arises only from the induced-dipole–induced-dipole interaction and is given by eq 13, where D_N is a geometrical constant depending on how

$$E_m{}^s = \frac{D_N}{r_d{}^3}\left(\frac{e\alpha C_i}{r_d{}^2}\right)^2 \tag{13}$$

the N CH fragments are arranged at the surface of the cavity. In both (12) and (13) a point molecule approximation is used. The energies E_q and $E_m{}^l + E_e{}^l$ are the same as in the microdipole model.

TABLE XII. Results on Nonpolar Systems:[a] Comparisons between the FKY Microdipole Model and the Nishida[b] Model for the Solvated Electron in Nonpolar Media

model	system	N	$V_0{}^e$	$r_d{}^{0\,c}$	$C_{1s}{}^d$	$C_{2p}{}^d$	hv calcd	hv exptl[f]	f^g
FKY	CH_2	4	0.5	2.25	0.2092	0.0006	0.426		
	fragments	8	0.0	2.74	0.1439	0.0015	0.168		
Nishida	3MP	4	1.20	2.01	0.242	0.001	0.717	0.73	0.234
		8	1.20	2.10	0.247	0.001	0.803		0.213
KFNK	3MP	4	0.60	4.2	0.756	0.038	0.605		0.364
		8	0.60	5.0	0.785	0.132	0.623		0.568

model	system	N	E_k	$E_e{}^s$	$E_m{}^s$	$E_e{}^1$	$E_m{}^1$	E_v	E_q	E_c	E_{HH}	E_t	$V_0 - E_t(1s)^i$
						Ground 1s State[h]							
FKY	CH_2	4	0.6513	-0.2548	0.0722	-1.7200	0.8600	0.0817	0.3570			0.0473	0.4527
	fragments	8	0.2913	0.1918	0.1706	-1.1794	0.5897	0.1212	0.0000			-0.2083	0.2083
Nishida	3MP	4	0.679	-0.067	0.006	-2.014	1.007	0.127	0.910	-0.177		0.471	0.729
		8	0.636	-0.088	0.015	-1.948	0.974	0.139	0.904	-0.237		0.395	0.805
KFNK	3MP	4	1.099	-1.052	0.169	-1.026	0.513	0.089	0.191		0.113	0.096	0.904
		8	0.775	-0.882	0.270	-0.916	0.458	0.324	0.178		0.069	0.276	0.724
						Excited 2p State[h]							
FKY	CH_2	4	0.1102	-0.0008	0.0104	-0.4496	0.2259	0.0756	0.4995			0.4737	
	fragments	8	0.1078	-0.0023	0.0321	-0.4395	0.2216	0.1212	0.0000			0.0408	
Nishida	3MP	4	0.140	-0.000	0.000	-1.102	0.551	0.127	1.199	-0.002		1.188	
		8	0.140	-0.000	0.000	-0.551	0.276	0.139	1.198	-0.003		1.198	
KFNK	3MP	4	0.276	-0.007	0.001	-0.732	0.366	0.089	0.930		0.113	1.036	
		8	0.685	-0.181	0.067	-0.878	0.439	0.324	0.590		0.069	1.116	

[a] See ref 72; all energies are in eV and distances are in Å. [b] See ref 73. [c] Distance between the center of the cavity and the nearest carbon atom. It is the value at the configurational minimum. [d] Excess electron charge density enclosed with the radius $r_d{}^0$. [e] In Nishida's model the V_0 values are experimental values taken from ref 55. [f] L. Kevan, *Adv. Radiat. Chem.*, 4, 181 (1974). [g] Oscillator strength. [h] Various energy terms used in the FKY model are adopted here, although there are some differences in the $E_e{}^s$ and $E_m{}^s$ terms in the two models (see text). [i] $V_0 - E_t(1s)$ gives a measure of the localization stability of the excess electron. See T. Kimura, K. Fueki, P. Narayana, and L. Kevan, *Can. J. Chem.*, 55, 1940 (1977).

The exchange interaction energy between the carbon core and the excess electron is given by eq 14, where $\chi_{\mu j}$ is the wave

$$E_{ex}{}^s = -e^2 \sum_{\mu=1}^{N} \int \left[3\alpha_C \left(\frac{8}{3\pi} \sum_j \chi_{\mu j}{}^2 \right)^{1/3} \right] \Psi_j d\tau \quad (14)$$

function of the jth core electron of the carbon atom located at the center of the μth nearest neighbor CH fragment. This energy was calculated using Slater's free electron approximation with a correction factor α_C and approximating $\chi_{\mu j}$ by a 1s Slater orbital. Nishida found this exchange energy to be relatively large in the ground state and essentially negligible for the more diffuse excited state. This could be an important point, but it is cautioned that the evaluation of this exchange energy is highly approximate, more so than the other energy terms in the model. Carmichael[64] has evaluated (14) numerically for Nishida's parameters for the ground state and finds values four- to fivefold smaller. He has also drawn attention to the fact that accurate calculation of the exchange interaction probably requires the excess wavefunction to be orthogonalized to the carbon cores.

The results of Nishida's model for electrons in 3-methylpentane are included in Table XII for comparison. In the original paper[62b] the results for electrons in methylcyclohexane are also given. The values for $V_0 - E_t(1s)$ at $N = 4$ and 6 are larger than the corresponding ones for the FKY microdipole model. These values are comparable to those obtained for some of the less polar media such as methyltetrahydrofuran, triethylamine, etc., but smaller than those in a polar system such as water by more than a factor of two. The source of the difference in $V_0 - E_t(1s)$ can be traced by examining the various energy terms. All the terms that appear in both models are comparable in magnitude except $E_{ex}{}^s$, $E_m{}^s$, and E_q. The increase in E_q is due to the V_0 value used. The exchange term E_{ex} plus the short-range electronic energy of eq 12 in Nishida's model give similar values to $E_e{}^s$ in the FKY model. Consequently, the main difference between the two models is in $E_m{}^s$. In Nishida's model the
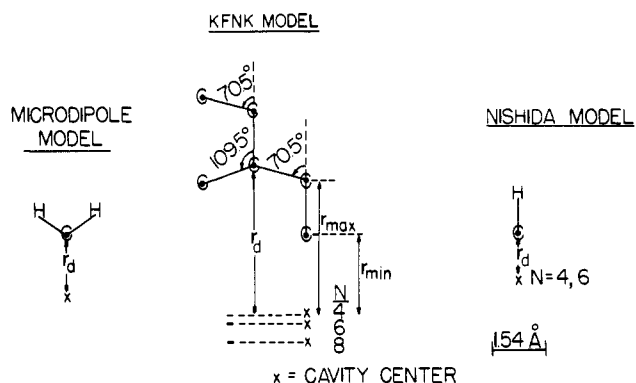

Figure 12. Comparisons between the FKY[61] microdipole, KFNK,[63] and Nishida models[62] for the localized electron in the nonpolar medium, 3-methylpentane.

dipole–dipole repulsive energy between the oriented dipoles is assumed to be compensated by the decreased energy between the electron and these dipoles. However, in the FKY microdipole model all pairwise CH_2 dipoles are included explicitly, and consequently an overestimation of the dipole repulsion is to be expected. When the nonequilibrium 2p excited state is calculated, Nishida's model can account for nearly the observed optical transition energy. Although the total energy between the two models is different, the physical features are surprisingly similar. For example, the distance between the cavity center and the nearest carbon atom is similar (see Table XII or Figure 12). The charge distribution of the excess electron enclosed within this distance is also quite similar for both the ground 1s and excited 2p states.

As pointed out earlier, electrons in most of the nonpolar media studied all absorb light in approximately the same region. This makes the comparisons between the calculated hv (1s → 2p) and the experimental hv_{max} an even less sensitive test of the

model than in polar systems. A more valid comparison may be how well the stability criterion $V_0 - E_t(1s)$ correlates with electron mobility data.

The widely varying electron mobilities in alkanes suggested to Kimura et al.[63] that the explicit molecular structure of the molecules solvating the electron must be incorporated in any realistic model of electron binding in alkanes. To accomplish this, the polarization of the solvent molecule is assumed to be distributed over the C–C bonds in each molecule. If there is one C–C bond, then the interaction potential for the ith electronic state between the electron and the jth C–C polarized bond of finite length is given by eq 15, where n is the number of C–C

$$V_j(i) = -\frac{\alpha e^2}{6nl \cos \theta_j}\left(\frac{1}{r_{j^3(\text{min})}} - \frac{1}{r_{j^3(\text{max})}}\right)C_i(r_{j0}) \quad (15)$$

bonds in the molecule, l is the C–C bond length, α is the polarizability of the medium molecule, θ is the angle between the jth C–C bond and a specifically defined radial direction, and $r_{j(\text{min})}$ and $r_{j(\text{max})}$ are the minimum and maximum of this radial distance of the projected jth bond. Figure 10 clearly shows the exact definition of these three parameters for a particular orientation of the 3-methylpentane molecule. C is the charge distribution of the electron enclosed within the distance r_{j0}. Within the framework of the semicontinuum model, this potential yields the short-range electronic energy where N is the number of solvent

$$E_e^s(i) = \sum_j NV_j(i)C_i(r_{j0}) \quad (16)$$

molecules in the first solvation shell. The short-range medium rearrangement energy is given by eq 13.

Since the number of hydrogens in alkanes is considerably greater than that in the polar systems, H_2O or NH_3, H–H repulsions are anticipated to be greater and thus an E_{HH} term is added to the total energy. The E_{HH} term is approximated by the expression

$$E_{HH}(\text{eV}) = \sum_h g_h \times 434 \exp(-4.6r_h) \quad (17)$$

where g_h is the number of hydrogen atom pairs separated by a distance $r_h(\text{Å})$.

By use of the various appropriate physical parameters and other geometrical constants that determine physically reasonable conformations of the first shell solvent molecules, the energy of the excess electron is calculated by minimization with respect to the trial wave function parameter. A configurational coordinate diagram is obtained for each system when the energy is minimized at various cavity radii r_d. The calculated results reveal that good agreement is obtained between calculated $h\nu(1s \rightarrow 2p)$ and experimental values. More importantly, when $V_0 - E_t(1s)$ values for different systems are calculated, the ground-state stability of the excess electron correlates very well with that inferred from electron mobility data. The larger the electron mobility, the more delocalized is the electron in the conduction state and, therefore, the smaller is $V_0 - E_t(1s)$. For comparison, the geometries of the KFNK,[63] FKY,[61] and Nishida[62] models are shown in Figure 12 for electrons in 3-methylpentane; the actual molecular geometry is only utilized in the KFNK model.

The results obtained from the KFNK structured semicontinuum model correlate well with experimental data. The model also accounts for the blue shift of the solvated electron spectra as observed by pulse radiolysis in deuterated liquid propane as the temperature is decreased.[65]

7. Current Problems

There are several current problems in solvated electron theory which deserve attention. Now that the detailed geometrical structure of solvated electrons is known, at least in aqueous systems,[25] more attention should be paid to understanding this
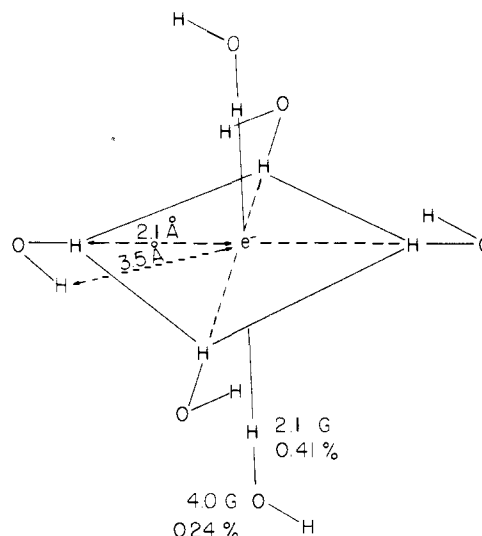
Figure 13. Geometrical structure of the solvated electron in aqueous glasses determined from electron spin–echo modulation magnetic resonance data. The isotropic hyperfine couplings to H and ^{17}O are given along with the corresponding percentage of solvated electron spin density on these atoms.

structure theoretically. A second major problem is how to explain the width of the optical absorption line. The existing theoretical models discussed in previous sections all predict a line shape that is too narrow and symmetric compared to experiment. A third related problem is how to calculate solvated electron tunneling rates[66,67] to scavengers for which there now exist much data.[68] We briefly discuss the first two problems in this section.

7.1. Molecular Geometry of Solvated Electrons

In the semicontinuum model the first solvation shell molecules are represented by point dipoles, so no detailed geometrical information is obtained. It has generally been assumed that the molecular dipoles of the first solvation shell molecules are at least approximately oriented toward the excess electron. This would certainly be the case if the electron were a point charge and the first solvation shell polar molecules were far enough removed to be well approximated as point dipoles. However, the solvated electron wave function extends to some extent over its first solvation shell. So if the electron–molecule interactions are strong enough, chemical forces such as exchange will come into play to affect the geometry of the solvated electron.

We can conceive of two limiting geometries for solvated electrons in polar media. In one the molecular dipoles of the solvent molecules are oriented toward the electron and in the other a polar or hydrogen bond of the solvent molecules is oriented toward the electron. Current electron magnetic resonance experiments are giving the first detailed experimental geometries of solvated electrons in different media[25,69,70] which provide benchmarks for theoretical comparison. Two contrasting cases are the geometries of solvated electrons in water[25] and ethanol.[70] In water the electron is surrounded by six waters arranged with one OH bond of each water oriented octahedrally about the electron with an electron to proton distance of 2.1 Å, as shown in Figure 13. So the molecular dipole of water is *not* oriented toward the electron. In ethanol the electron is surrounded tetrahedrally by *four* ethanols arranged with their molecular dipoles, which approximately bisect the COH bond angle,[71] oriented toward the electron; the orientation of a single ethanol molecule with respect to the electron is shown in Figure 14. The theoretical challenge is to account for these differences.

The solvation geometry can be explored theoretically by molecular orbital methods and by the "ab initio" semicontinuum
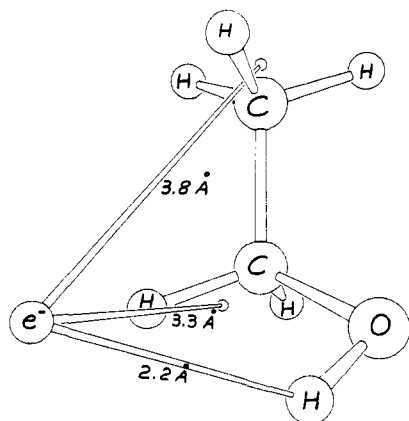
Figure 14. Suggested orientation of an individual first solvation shell molecule with respect to the solvated electron in ethanol from electron spin–echo data.[70] The distances are average distances to the OH, CH_2, and CH_3 protons. The entire solvation shell includes four ethanol molecules so oriented and arranged tetrahedrally around the electron. The molecular dipole of ethanol approximately bisects the COH angle and can be seen to be oriented approximately toward the electron.

Figure 15. Theoretical line shape for the ammoniated electron as calculated by the CKJ semicontinuum model.[39]

model. Calculations to date have only been done for water and usually only for tetrahedral geometries. Howat and Webster[8b] used the INDO approximation to compare OH-bond-oriented and molecular-dipole-oriented tetrahedral geometries for water. They found that the OH-bond-oriented geometry had lower energy but, of course, the whole solvated electron system is unstable in that approximation. Noell and Morokuma[21] compared a molecular-dipole-oriented tetrahedral geometry with a bond-oriented octahedral geometry for water in their fractional charge molecular orbital model. Again the entire system is unstable, but given a specific neutral arrangement of waters they found the bond-oriented geometry to be more stable. In the "ab initio" semicontinuum model of Newton[5] both bond- and dipole-oriented tetrahedral geometries were considered. In this model the solvated electron is stable and the dipole-oriented geometry is slightly more stable. These results do not suggest that the existent theory can "predict" the experimental solvation geometry, but no theoretical studies specifically directed toward the geometry problem, in light of the new experimental data, have yet been made.

7.2. Optical Absorption Line Shape

It is well-known that the optical absorption spectrum of the solvated electron in glasses or liquids is broad, structureless, and asymmetric toward the high-energy side. Regardless of the medium, all spectra are very similar in shape although the energy of the maximum differs. The gross features of the spectrum, such as the optical absorption maximum as a function of matrix polarity, temperature, pressure, is quite well understood. However, the simulation of the line shape directly from existing models still poses some problems.

Both the FFK and CKJ models can only account for less than half of the experimental line width. More disturbing is the fact that the simulated line shape is approximately symmetric rather than skewed toward the high-energy side of the spectrum, as found experimentally. Kestner and Jortner[52] explored this problem with a temperature-independent potential and calculated the total ground- and excited-state energies as a function of both the cavity radius and the dipole orientation angle. They called this the two-coordinate model. The results obtained in this manner are thermally averaged by introducing a Boltzmann weighted factor. The results are very similar to the effect of a Langevin function incorporated in the short-range charge–dipole potential and the dipole–dipole repulsion term. The broadening effect on the line shape is still small and the asymmetry is in the wrong direction.
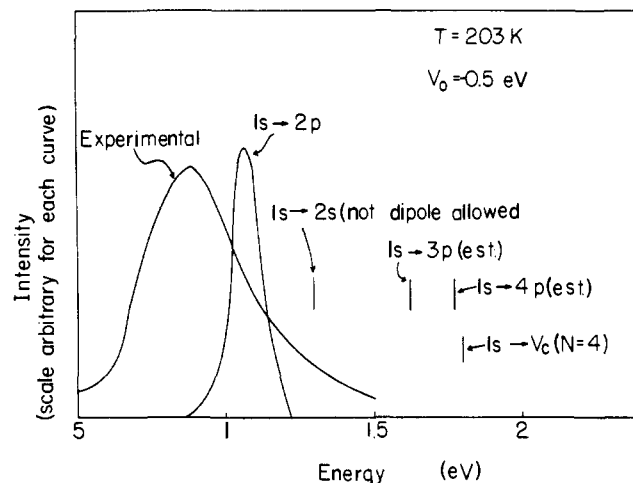
Gaathon and Jortner suggested[72] that the spectral width may be associated with a distribution of solvation shell sizes with 4, 6, and 8 molecules, for example. Experimentally one might then expect to see a significant broadening of the line width as the density increases. However, experimental studies indicate very little difference in the line width as the density is changed.[73] Also the calculation of a composite spectrum of $N = 4$ and $N = 6$ does indeed show that the calculated line width is still well below the experimental one.

Another possibility is that the line width reflects transitions to higher bound states. This would broaden the spectrum on the high-energy side. Kestner[39] examines 1s $\rightarrow$ 3p, 1s $\rightarrow$ 4p, and 1s $\rightarrow$ continuum transitions by assuming that these higher states can be represented by the Rydberg formula. Unfortunately, these transitions are too high in energy and also the corresponding oscillator strengths are too small to broaden the principal 1s $\rightarrow$ 2p line. Numerical solutions of the semicontinuum model also support this conclusion.[56] The role of solvent vibrational modes on the ground-state energy was also estimated assuming harmonic motion, but the line broadening remains unsufficient. Figure 15 summarizes these studies on the line-shape problem for the solvated electron in liquid ammonia.

A variation on the idea of incorporating higher bound states to explain the optical band shape is to assume a statistical distribution of trap depths in a semicontinuum model framework.[74] Such a model can account for the optical band width of solvated electrons at the expense of adding two additional parameters characterizing the distribution of cavity sizes and short-range interaction energies. However, the physical significance of such a model is unclear.

Tachiya et al.[75] also examined the line-shape problem based on the simpler continuum model.[9] There the hydrated electron spectrum is simulated by calculating the 1s $\rightarrow$ 2p transition energy with different fractions of orientational polarization. With this method the spectrum obtained is still symmetrical.

By adjusting a spherical well in such a way that only one bound state is obtained, Kajiwara et al.[76] and Huang et al.[77] simulated the bound–continuum band shape for the solvated electron in ammonia, water, and alcohol. In general, these photoionization spectra agree well with the experimental line shape. Mazzacurati et al.,[78] using an exact absorbance expression for an electron trapped in a spherical cavity, also obtained good agreement. Although the potential is not very realistic and the long-range interactions are completely ignored, recent photoemission spectroscopic data do support a significant photoionization contribution to the optical spectrum.[79] Fueki et al.[80] employed a hydrogenic model for the photoionization probability, used parameters calculated from the semicontinuum model, and

obtained bound–free spectral shapes for electrons in several polar media. Their results are in reasonable agreement with the wavelength dependence of photobleaching and photoconductivity in these systems.

In the above models the Hamiltonian of the excess electron system is simplified by including only the motion of the excess electron. The effect of the vibrational motion of the solvent molecules is added in an ad hoc fashion after the calculation of the electronic motion to try to account for the spectral width. Banerjee and Simons[81] have attacked the problem more rigorously by starting with a Hamiltonian which includes both the electronic and the vibrational motions of the entire system of electron plus solvent molecules. Their new feature is that they treat both the electronic and vibrational motions in a unified fashion. They use this Hamiltonian to develop quite general expressions for the time-correlation function of the dipole moment operator, $\langle F(t)f(0) \rangle$. The Fourier transform of this function formally gives the absorption band-shape function, $I(\omega)$, through eq 18. This theory appears intimidatingly formal, but the authors

$$I(\omega) = (2\pi)^{-1} \int_{-\infty}^{+\infty} e^{i\omega t} dt \langle F(t)F(0) \rangle \qquad (18)$$

have made a number of simplifying approximations to enable them to apply it to solvated electrons in ethanol and anthracene. They finally obtain $I(\omega)$ as a sum of three contributions. The largest contribution corresponds to a localized transition. This is similar to that considered in semicontinuum models with the addition of Franck–Condon factors for coupling of vibrational motions. The other contributions correspond to nonlocalized transitions which include transitions from the ground state of one site to excited states of neighboring sites. These contributions are equivalent to electron-hopping transitions. It is the contributions from these nonlocalized transitions which can formally account for the skewedness of the optical band.

The simplified theoretical expressions contain nine parameters which are determined by fitting a simulated band shape to the experimental one. These parameters include the fundamental frequency, the threshold frequency for the absorption, two geometrical displacement parameters, the localized dipole transition amplitude, the ratio of the nonlocalized to the nonlocalized plus localized dipole transition amplitude, the width of the inhomogeneous broadening, and two fluctuation parameters. It is not surprising that a fit to the experimental spectrum is achieved with this many remaining parameters. Also, the question of the uniqueness of the parameters deduced remains to be explored.

The critical point is not that a fit is achieved, but what physical insight about the band shape can be gained from this theory in its present form. The physical basis for the spectral width does not yet seem to be succinctly elucidated. However, the skewedness to high energy depends physically on contributions from nonlocalized transitions. Such contributions seem to imply that the solvated electrons have a finite probability of hopping from site to site. Furthermore, it would seem that this probability is greater on the high-energy side of the spectrum. If so, this model bears some physical similarity to a semicontinuum model involving both bound–bound and bound–continuum transitions which can also fit the solvated electron band shape.[80]

The formal model of Banerjee and Simons[81] is impressive. Further work on its application to a variety of solvent systems is necessary to show whether its derived parameters show physically sensible trends and to clarify its physical implications concerning the band shape.

8. Concluding Remarks

The CKJ and FFK semicontinuum model appears to be a reasonably successful theoretical model for treating the energy

level structure of solvated electrons. It is particularly useful because it is simple enough to apply to a wide variety of solvent systems at different temperatures and pressures. It is successful at predicting many experimental trends.

Nevertheless, the model has demonstrated defects both in the potential[14] and in the wave functions[56] used. The potential is too long range and the wave functions are too diffuse.

It is necessary to use the ab initio semicontinuum model to study the geometrical structure of solvated electrons. Since good experimental data now exist for solvated electrons in, at least, water and ethanol with greatly contrasting geometries, it is possible to test the success of the ab initio model for treating geometry. However, the ab initio modification of the CKJ and FFK semicontinuum model makes it expensive and time consuming to apply.

The semicontinuum model is notably unsuccessful in treating the optical absorption band shape. A number of other models have been proposed, some of which claim successful fits. In all cases it appears that some contribution from bound–continuum transitions must be invoked. This seems consistent with experiment. However, none of the theories have yet been able to give a clear physical basis for the observed line shape.

The development of solvated electron theory has depended on a continual and exciting interplay between experiment and theory. Many physical and chemical advances have been made with fallout into various other scientific fields. This interplay must be continued for future advancement in our knowledge of localized electrons in condensed media.

9. References

(1) L. Kevan, *Adv. Radiat. Chem.*, **4**, 181 (1974).
(2) L. Kevan, *J. Phys. Chem.*, **76**, 3830 (1972).
(3) For example, (a) L. Kevan, "Radiation Research", Academic Press, New York, 1975, p 406; (b) for liquid: D. Huppert, W. S. Struve, P. Reutzepis, and J. Jortner, *J. Chem. Phys.*, **63**, 1205 (1975); (c) for solid: L. Kevan, *ibid.*, **56**, 838 (1972).
(4) (a) R. A. Ogg, *Phys. Rev.*, **69**, 243 (1933); (b) W. N. Lipscomb, *J. Chem. Phys.*, **21**, 52 (1953).
(5) M. Newton, *J. Chem. Phys.*, **58**, 5833 (1973); *J. Phys. Chem.*, **79**, 2795 (1975).
(6) C. A. Naleway and M. E. Schwartz, *J. Phys. Chem.*, **76**, 3905 (1972).
(7) (a) J. A. Pople and D. L. Beveridge, "Approximate Molecular Orbital Theory", McGraw-Hill, New York, 1970; (b) J. N. Murrell and A. J. Harget, "Semi-empirical Self-Consistent-Field Molecular Orbital Theory of Molecules", Wiley-Interscience, New York, 1972.
(8) (a) B. C. Webster and G. Howat, *Radiat. Res. Rev.*, **4**, 259 (1972); (b) G. Howat and B. C. Webster, *J. Phys. Chem.*, **76**, 3714 (1972); (c) B. J. McAloon and B. C. Webster, *Theor. Chem. Acta*, **15**, 385 (1969); (d) M. Weissmann and N. V. Cohan, *Chem. Phys. Lett.*, **7**, 445 (1970); *J. Chem. Phys.*, **59**, 1385 (1973).
(9) (a) J. Jortner, *Mol. Phys.*, **5**, 257 (1962); (b) *Radiat. Res., Suppl.*, **4**, 24 (1964); (c) *J. Chem. Phys.*, **30**, 839 (1959).
(10) D. Copeland, N. R. Kestner, and J. Jortner, *J. Chem. Phys.*, **53**, 1189 (1970).
(11) K. Fueki, D. F. Feng, and L. Kevan, *J. Phys. Chem.*, **74**, 1976 (1970).
(12) K. Fueki, D. F. Feng, and L. Kevan, *J. Am. Chem. Soc.*, **95**, 1398 (1973).
(13) T. Kimura, K. Fueki, P. Narayana, and L. Kevan, *Can. J. Chem.*, **55**, 1940 (1977).
(14) N. R. Kestner, *Can. J. Chem.*, **55**, 1937 (1977).
(15) (a) S. Ishimaru, T. Yamabe, K. Fukui, and H. Kato, *Chem. Phys. Lett.*, **17**, 264 (1972); (b) *J. Phys. Chem.*, **77**, 1450 (1973).
(16) L. Raff and H. A. Pohl, *Adv. Chem. Ser.*, **No. 50**, 173 (1965).
(17) D. Park, "Introduction to the Quantum Theory", McGraw-Hill, New York, 1964, Chapter 16.
(18) J. L. Whitten, *J. Chem. Phys.*, **39**, 249 (1963).
(19) J. L. Whitten, *J. Chem. Phys.*, **44**, 359 (1966).
(20) S. Ray, *Chem. Phys. Lett.*, **11**, 573 (1971).
(21) J. O. Noell and K. Morokuma, *J. Phys. Chem.*, **81**, 2295 (1977).
(22) A. Ben-Naim, "Water and Aqueous Solutions", Plenum Press, New York, 1974, p 243.
(23) B. L. Bales, J. Helbert, and L. Kevan, *J. Phys. Chem.*, **78**, 221 (1974).
(24) B. L. Bales, M. K. Bowman, L. Kevan, and R. N. Schwartz, *J. Chem. Phys.*, **63**, 3008 (1975).
(25) S. Schlick, P. A. Narayana, and L. Kevan, *J. Chem. Phys.*, **64**, 3153 (1976).
(26) L. Kevan, M. K. Bowman, P. A. Narayana, R. K. Boeckman, V. F. Yudanov, and Yu. D. Tsvetkov, *J. Chem. Phys.*, **63**, 409 (1975).

(27) P. A. Narayana, M. K. Bowman, L. Kevan, V. F. Yudanov, and Yu. D. Tsvetkov, *J. Chem. Phys.*, **63**, 3365 (1975).
(28) M. Natori and T. Watanabe, *J. Phys. Soc. Jpn.*, **21**, 1573 (1966).
(29) M. Natori, *J. Phys. Soc. Jpn.*, **24**, 913 (1968).
(30) M. Natori, *J. Phys. Soc. Jpn.*, **27**, 1309 (1969).
(31) L. Landau, *Phys. Z. Sowjetunion*, **3**, 664 (1933).
(32) K. Fueki, *J. Chem. Phys.*, **44**, 3140 (1966).
(33) B. G. Ershov, I. E. Makarov, and A. K. Pikaev, *High Energy Chem.*, **1**, 414 (1967).
(34) K. Fueki, D. F. Feng, and L. Kevan, *Chem. Phys. Lett.*, **4**, 313 (1969).
(35) I. Carmichael and B. Webster, *J. Chem. Soc.*, **70**, 1570 (1974).
(36) K. Iguchi, *J. Chem. Phys.*, **48**, 1735 (1968).
(37) K. Iguchi, *J. Chem. Phys.*, **51**, 3137 (1969).
(38) K. Fueki, D. F. Feng, L. Kevan, and R. Christofferson, *J. Phys. Chem.*, **75**, 2297 (1971).
(39) N. R. Kestner in "Electron-Solvent and Anion Solvent Interactions", L. Kevan and B. Webster, Eds., Elsevier, Amsterdam, 1976, Chapter 1.
(40) B. E. Springett, J. Jortner, and M. H. Cohen, *J. Chem. Phys.*, **48**, 2720 (1968).
(41) M. Cohen and J. Lekner, *Phys. Rev.*, **158**, 305 (1967).
(42) S. Noda and L. Kevan, *J. Chem. Phys.*, **61**, 2467 (1974).
(43) S. Noda, L. Kevan, and K. Fueki, *J. Phys. Chem.*, **79**, 2866 (1975).
(44) R. A. Holroyd and M. Allen, *J. Chem. Phys.*, **54**, 5014 (1971).
(45) R. A. Holroyd, *J. Chem. Phys.*, **57**, 3007 (1972).
(46) W. Tauchert, H. Jungblut, and W. F. Schmidt, *Can. J. Chem.*, **55**, 1860 (1977).
(47) D. Grand, A. Bernas, and E. Amouyal, *Chem. Phys.*, in press.
(48) J. Helbert, L. Kevan, and B. L. Bales, *J. Chem. Phys.*, **57**, 723 (1972).
(49) (a) U. Schindewolf, *Angew. Chem., Int. Ed. Engl.*, **6**, 575 (1967); (b) U. Schindewolf, H. Kohrmann, and G. Lang, *ibid.*, **8**, 512 (1969).
(50) R. R. Hentz, Farhataziz, and E. M. Hansen, *J. Chem. Phys.*, **55**, 4974 (1971).
(51) M. G. Robinson, K. N. Jha, and G. R. Freeman, *J. Chem. Phys.*, **55**, 4933 (1971).
(52) N. R. Kestner, J. Jortner, and A. Gaathon, *Chem. Phys. Lett.*, **19**, 328 (1973).
(53) K. Fueki, D. F. Feng, and L. Kevan, *J. Phys. Chem.*, **78**, 393 (1974).
(54) H. Hase, M. Noda, and T. Higashimura, *J. Chem. Phys.*, **54**, 2975 (1971).
(55) K. Fueki, D. F. Feng, and L. Kevan, *J. Chem. Phys.*, **58**, 5351 (1972).
(56) (a) B. C. Webster and I. Carmichael, *J. Chem. Phys.*, **68**, 4086 (1978); (b) B. C. Webster, *J. Chem. Soc., Faraday Trans. 2*, **73**, 1699 (1977); (c) I. Carmichael, *J. Phys. Chem.*, in press.
(57) D. F. Feng, D. Ebbing, and L. Kevan, *J. Chem. Phys.*, **61**, 249 (1974).
(58) M. Magat, *Ber. Bunsenges. Phys. Chem.*, **75**, 666 (1971).
(59) P. A. Narayana and L. Kevan, *J. Chem. Phys.*, **65**, 3379 (1976).
(60) W. Schmidt in "Electron-Solvent and Anion-Solvent Interactions", L. Kevan and B. Webster, Eds., Elsevier, Amsterdam, 1976, Chapter 7.
(61) D. F. Feng, L. Kevan and H. Yoshida, *J. Chem. Phys.*, **61**, 4440 (1974).
(62) (a) M. Nishida, *J. Chem. Phys.*, **65**, 5242 (1976); (b) M. Nishida, *ibid.*, **66**, 2760 (1977); (c) M. Nishida, *ibid.*, **67**, 4786 (1977).
(63) T. Kimura, K. Fueki, P. A. Narayana, and L. Kevan, *Can. J. Chem.*, **55**, 1940 (1977).
(64) I. Carmichael, private communication.
(65) L. Kevan, H. Gillis, K. Fueki, and T. Kimura, *J. Chem. Phys.*, **68**, 5203 (1978).
(66) I. Webman and N. R. Kestner, *J. Phys. Chem.*, **83**, 451 (1979).
(67) W. M. Bartczak, J. Kroh, and Cz. Stradowski, *J. Chem. Phys.*, **66**, 2737 (1977).
(68) J. R. Miller, *J. Phys. Chem.*, **82**, 767 (1978).
(69) T. Ichikawa, L. Kevan, M. K. Bowman, S. A. Dikanov, and Yu. D. Tsvetkov, *J. Chem. Phys.*, **71**, 1167 (1979).
(70) M. Narayana and L. Kevan, *J. Chem. Phys.*, in press.
(71) E. V. Ivash and D. M. Dennison, *J. Chem. Phys.*, **21**, 1804 (1979).
(72) A. Gaathon and J. Jortner, "Electrons in Fluids", J. Jortner and N. R. Kestner, Eds., Springer-Verlag, New York, 1973, p 429.
(73) R. Olinger, U. Schindewolf, A. Gaathon, and J. Jortner, *Ber. Bunsenges Phys. Chem.*, **75**, 690 (1971).
(74) W. M. Bartczak, M. Hilczer, and J. Kroh, *J. Phys. Chem.*, in press.
(75) M. Tachiya, Y. Tabata, and K. Oshima, *J. Phys. Chem.*, **77**, 263 (1973).
(76) Kajiwara, K. Funabashi, and C. Naleway, *Phys. Rev. A*, **6**, 808 (1972).
(77) J. T. Huang and F. O. Ellison, *Chem. Phys. Lett.*, **28**, 189 (1974).
(78) V. Mazzacurati and G. Signorelli, *Lett. Nuovo Cimento*, **12**, 347 (1975).
(79) P. Delahay, "Electron-Solvent and Anion-Solvent Interactions", L. Kevan and B. Webster, Eds., Elsevier, Amsterdam, 1976, Chapter 4.
(80) K. Fueki, D. F. Feng, and L. Kevan, *J. Chem. Phys.*, **59**, 6201 (1973).
(81) A. Banerjee and J. Simons, *J. Chem. Phys.*, **68**, 415 (1978).